Journal of Anthropological Archaeology 79 (2025) 101711

Contents lists available at ScienceDirect

Journal of Anthropological Archaeology

journal homepage: www.elsevier.com/locate/jaa

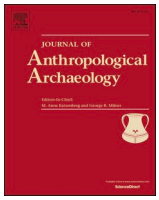

Raised from the ashes: Geoarchaeological perspectives on house burning practices in an Iberian Iron Age village

Laura Tomé [a,b,*], Antonio Blanco-González [c], Eneko Iriarte [d], Ángel Carrancho [e], Natalia García-Redondo [f], Santiago Sossa-Ríos [g], Alejandra Sánchez-Polo [h], María Martín-Seijo [i], Carolina Mallol [a,b,j,*]

[a] Archaeological Micromorphology and Biomarkers Laboratory (AMBI Lab), Instituto Universitario de Bio-Orgánica "Antonio González", Universidad de La Laguna, 38206 Tenerife, Spain
[b] Área de Prehistoria, Departamento de Geografía e Historia, Facultad de Humanidades, Universidad de La Laguna, 38206 Tenerife, Spain
[c] Research Group PREHUSAL, Departamento de Prehistoria, Historia Antigua y Arqueología, Facultad de Geografía e Historia, Universidad de Salamanca 37002 Salamanca, Spain
[d] Laboratorio IsoTOPIK-Laboratorio de Evolución Humana, Departamento de Historia, Geografía y Comunicación, Facultad de Humanidades y Comunicación, Universidad de Burgos 09001 Burgos, Spain
[e] Área de Prehistoria, Departamento de Historia, Geografía y Comunicación, Universidad de Burgos 09001 Burgos, Spain
[f] Laboratorio de Paleomagnetismo, Departamento de Física, Universidad de Burgos 09006 Burgos, Spain
[g] Departament de Prehistòria, Arqueologia i Historia Antiga, Universitat de València. Avinguda Blasco Ibañez 28, 46010 València, Spain
[h] Research Group PREHUSAL, Departamento de Prehistoria, Arqueología, Antropología, CC.TT. Historiográficas, Facultad de Filosofía y Letras, Universidad de Valladolid 470100 Valladolid, Spain
[i] Instituto de Ciencias del Patrimonio (INCIPIT), Consejo Superior de Investigaciones Científicas (CSIC), Edificio Fontan, Bloque 4, Monte Gaias, s/n. 15707 Santiago de Compostela, Spain
[j] Interdisciplinary Center for Archaeology and the Evolution of Human Behaviour (ICArEHB), Universidade do Algarve, Campus de Gambelas, Edifício 1, 8005-139 Faro, Portugal

ARTICLE INFO

Keywords:
Geoarchaeology
Micromorphology
Early Iron Age
House burning
Household archaeology
Earthen architecture

ABSTRACT

Burnt houses are a recurrent phenomenon in the prehistoric archaeological record, yet the specific processes behind their burning—likely varying across time and place—remain poorly understood. This study focuses on a thoroughly studied dwelling (House 1) from the Iberian Early Iron Age settlement of Cerro de San Vicente and investigates site formation processes associated with its burning. To achieve this, we applied a multi-proxy geoarchaeological approach, integrating archaeological soil micromorphology—including charcoal analysis on thin sections—, magnetic properties analyses, XRD, XRF, and GIS-based morphological and spatial analyses of mudbricks. Our results suggest that House 1 experienced a high temperature fire, reaching temperatures of up to ~700 °C, which destroyed its roof, burnt its walls, and generated an ash deposit rich in combustion residues. Shortly thereafter, the house was deliberately infilled with burnt reused mudbricks, recycled both from its dismantled walls and potentially other buildings across the settlement. This practice likely served to raise the level of the house to compensate for midden accumulation in the surrounding transit areas while providing a foundation for new construction phases. These findings suggest that construction materials were reused over time according to context-specific cultural rationales, potentially reflecting elements of a prehistoric circular economy. This research enhances our understanding of settlement and socio-cultural dynamics at Cerro de San Vicente, while contributing to broader archaeological discussions on the roles of prehistoric house burning practices.

* Corresponding authors at: Archaeological Micromorphology and Biomarkers Laboratory (AMBI Lab), Instituto Universitario de Bio-Orgánica "Antonio González", Universidad de La Laguna, 38206 Tenerife, Spain.
E-mail addresses: lhernant@ull.edu.es (L. Tomé), cmallol@ull.edu.es (C. Mallol).

https://doi.org/10.1016/j.jaa.2025.101711
Received 5 March 2025; Received in revised form 24 June 2025;
Available online 12 July 2025

1. Introduction

1.1. Formation and significance of destruction deposits

Destruction deposits are a common feature in archaeological contexts from the onset of sedentism and urbanization (Twiss et al. 2008; Namdar et al. 2011; Tringham 2013; Harvig et al. 2015; Regev et al. 2015; Amadio and Bombardieri 2019; Shahack-Gross 2020; Kovács et al. 2023; Runjajić et al. 2023; Shalom et al. 2023; Cutillas-Victoria et al. 2024), and often preserve valuable information about past critical, irreversible events (e.g., accidents, violent episodes, natural catastrophes, intentional destructions, etc.) (Driessen 2013a; Shahack-Gross 2020). Since the 1980s, understanding the dynamics and significance of destruction events has been a relevant debate in archaeology (Binford 1981; Schiffer 1985; Murray 1999), especially in efforts to discern whether their material correlates (i.e., destruction deposits) offer an accurate, representative high-resolution snapshot of past human societies.

Driessen (2013b) theorized about the characteristics that define eventful destruction deposits and their genesis. Destruction deposits in archaeological contexts often result from critical, highly irreversible events in which an external agent—commonly fire—is involved. As such, they frequently result in unintentional, thick deposits with high concentrations of archaeological materials. Drawing on Lucas' (2004, 2008) and Bailey's (2007) work on the temporality of archaeological deposits, Driessen (2013b) highlights that destruction layers may yield archaeological assemblages of increased spatial and temporal resolution: first, they act as stratigraphic temporal markers, because they exhibit very distinct depositional dynamics compared to regular occupation surfaces; second, these deposits are usually sealed rapidly, preventing any possible post-depositional disturbances that may occur after the destructive event. In addition, destructions usually act as immobilizers, preventing the reclamation and reuse of any objects or elements affected by the event. Considering all this, destruction layers would very likely preserve valuable information about the processes leading to their formation and the human activities involved—often more so than middens, constructed floors, or other occupation deposits.

Destruction deposits often pose significant challenges for archaeologists seeking an accurate understanding of past human behavior. These challenges include understanding the event's duration and impact, identifying the agents responsible for the destruction, and elucidating the formation processes involved in order to achieve a precise temporal and spatial comprehension of such phenomena (Driessen 2013b).

If destruction events—materialized in archaeological sites as *sedimentary* deposits—indeed offer a high spatial and temporal resolution view of past social practices, then high-resolution geoarchaeological techniques are required to address these questions. In fact, previous studies have successfully proven so through the application of combined geoarchaeological techniques in urban settings (Namdar et al. 2011; Regev et al. 2015; Sapir et al. 2018; Kreimerman et al. 2022; Runjajić et al. 2023; Shalom et al. 2023). However, while these cases focus on large-scale destructions in urban contexts, smaller, more localized deposits, constrained within single prehistoric dwellings, can also offer accurate information about past social and cultural dynamics. In fact, the burning and shattering of prehistoric houses has been a recurring research topic for decades (Bankoff and Winter 1979; Stevanović 1997; Chapman 1999; Tringham 2013; Balbo et al. 2012), as these events potentially offer valuable insights into past daily and communal social practices.

1.2. The conflagration of prehistoric houses

House burning has been a widespread phenomenon documented across various chronologies and geographical settings throughout prehistoric times. While it has been particularly studied in the context of the Neolithic and Copper Age in the Balkans—often referred to as the 'Burnt House Horizon' (*ca.* 5500–3500 BCE) (Tringham et al. 1992; Tringham 2013)—it has also been the focus of recent studies examining Neolithic to Iron Age contexts in diverse locations (Smith 1990; Webley 2007; Sánchez-Polo and Blanco-González 2014; Russell et al. 2014; Taylor et al. 2017; Harvig et al. 2015; Amadio and Bombardieri 2019; Blanco-González et al. 2022; Kovács et al. 2023).

For decades, researchers have sought to unravel the explanations behind this archaeological phenomenon (Bankoff and Winter 1979; Cessford and Near 2005; Stevanović 1997; Chapman 1999; Twiss et al. 2008; Harrison 2013). In this context, Sánchez Polo (2021) summarized the primary interpretations proposed to date, which include: 1) accidental burning (e.g., natural phenomena, domestic accidents), and 2) intentional firing. The latter encompasses various possibilities, such as violent conflicts between human groups, utilitarian practices (e.g., modifying construction materials through fire, cleaning, or fumigation), and/or the deliberate destruction of a house at the end of its life cycle, understood as symbolic/ritual behaviour. Such considerations have not only been made in Southeastern Europe but also in the Iberian Peninsula. Sánchez Polo (2021) established thirteen criteria to distinguish between intentional and accidental burning of prehistoric buildings and explored their implications for the Bronze Age in the Northern Iberian Plateau. Her research proposes that certain dwellings were deliberately and carefully set on fire in connection with special communal events, as part of cleansing rituals and prescriptive practices rooted in mythological traditions.

Although understanding such complex phenomena—and the specific cultural drivers behind them—requires addressing multiple variables that likely varied across archaeological contexts (Chapman, 1999), scholars have generally argued that house burning practices were often closely tied to social and communal dynamics within households (Chapman 1999; Sánchez Polo 2021; Stevanović 1997; Tringham 2013). First, the destruction of houses can be understood as a form of communal maintenance, undertaken once regular refurbishment activities were no longer sufficient for the dwelling's upkeep—potentially prompting the reuse of construction materials in new building phases (Brooks 1993; Shaffer 1993). Second, if these acts marked the end of a house's life cycle, its destruction—and subsequent rebuilding—would have signalled the start of a new phase of occupation atop the remains of the old (Driessen 2013a; Russell et al. 2014; Webley 2007). Scholars have argued that such practices may have served to reaffirm ties between the living and their ancestors, embedding social memory within the built environment (Chapman 1999). Thus, examining house burning practices offers a valuable lens through which to explore how households structured social continuity and reshaped their inhabited space over time (Kovács et al., 2023; Kruger, 2015; Matthews, 2016; Tringham, 2013; Twiss et al., 2008).

For the past decades, researchers have carried out various studies to explore the potential explanations behind house burning, including the ethnoarchaeological, experimental and monitored conflagration of dwellings (Bankoff and Winter 1979; Friede and Steel 1980; Shaffer 1993; Gheorghiu 2017, 2019; Johnston et al 2018, 2019; Kreimerman and Shahack-Gross 2019), the controlled burning of mudbricks and other earth-based construction materials (Gheorghiu 2008; Forget et al. 2015; Forget and Shahack-Gross 2016; Kreimerman and Shahack-Gross 2019) and geo-ethnoarchaeological analyses of recent burnt and decayed earthen dwellings (Friesem et al. 2014a, b; Kruger 2015; Friesem 2018). The direct application of geoarchaeological techniques to archaeological burnt dwellings has also been pivotal. For instance, Shaffer (1993) utilized archaeomagnetic analysis at Piana di Curinga (Italy), while Stevanović (1997) employed X-Ray Fluorescence (XRF), X-Ray Diffraction (XRD), and soil micromorphology at Opovo (Republic of Serbia), both focusing on burnt earthen materials. These studies determined the burning temperatures reached (above ~1000 °C) and the geochemical and mineralogical modifications undergone by earth-based construction materials. In a recent study, Kovács et al. (2023) implemented archaeological soil micromorphology, including phytolith

analysis on thin sections, to investigate an earthen building at the tell site of Százhalombatta-Földvár, Hungary. Their analysis confirmed the occurrence of a high-intensity fire at the end of the house's life cycle, which severely impacted the clay basin and wall plasters of the structure. Overall, these studies have provided valuable insights into the identification of burning events, the duration, temperatures and fuel required for a dwelling to be destroyed by fire, and the transformations undergone by earthen construction materials under such conditions.

Therefore, the application of geoarchaeological analyses to combustion deposits in prehistoric houses holds significant potential, as it provides deeper insights into formation processes, the transformations experienced by construction materials, the temporal framework of the destruction, and the duration of such events. In this paper, we applied a combination of high-resolution, microcontextual geoarchaeological techniques to an Early Iron Age dwelling at the site of Cerro de San Vicente (Salamanca, Spain), a settlement where several burnt houses have been documented to date (Blanco-González et al. 2017). Particularly, this study focuses on House 1, which exhibits evidence of burning with exceptional preservation, providing a unique opportunity to explore the potential of geoarchaeology in understanding prehistoric house-burning practices and their broader cultural implications.

1.3. *The case of House 1 at Cerro de San Vicente*

Cerro de San Vicente (hereafter CSV) is an Early Iron Age village (*ca.* 900–400 BCE) located in the Central Iberian Plateau (Spain), renowned for the remarkable preservation and highly-detailed excavation of several earthen dwellings (a more detailed description of the site is provided in Section 2.1). Among the dwellings documented at CSV, House 1 stands out as the most significant to date due to its exceptional archaeological relevance, making it the focus of previous studies (García-Redondo et al. 2021; Blanco-González et al. 2022; Tomé et al. 2024a; Chapon et al. 2024) (Fig. 1). It is a roundhouse of approximately 28 m^2, with preserved walls consisting of four courses of mudbrick laid lengthwise, reaching a maximum preserved height of 60 cm. The earthen dwelling features a central clay hearth, two built-in earthen benches against the wall, and a trapezoidal entrance hall added in a later construction phase (Fig. 2**A**). A test pit performed inside the roundhouse revealed a ~15 cm thick sequence of at least 30 microstratified clay floors and floor preparation layers (Tomé et al. 2024a). The central clay hearth was dated by full-vector archaeomagnetic dating and carrying out a multimethod archaeointensity approach, yielding an age range between 654 and 575 BCE at 2σ (García-Redondo et al. 2021).

During excavation, a charcoal-rich ashy layer was documented above the microstratified earthen floor sequence (Fig. 3**A** and Fig. 3**B**). That layer was ~4 cm thick, and covered the clay benches, the central clay hearth, and the most recent earthen floor (Blanco-González et al. 2022). The only archaeological items documented in association with such earthen floor were an iron knife, 17 quern fragments, and scattered pottery shards (Fig. 3**A** and Fig. 3**B**), often with signs of burning. These items are exceptional, as it is highly uncommon to recover any objects or fragments when this type of houses are excavated. Preliminary anthracological data indicated that *Pinus* tp. *pinea/pinaster* is the predominant taxon in the charcoal record, followed by *Quercus* sp. evergreen and *Cistus* sp. The charcoal fragments, together with the ash layer, were interpreted as the remains of the building materials from the walls and ceiling of the dwelling or either as possible fire-starters, affected by an intense burning event (Blanco-González et al. 2022). The temperature reached by such a fire inside House 1 must have been very high and sustained, as evidenced by the fact that the mud plaster still remaining

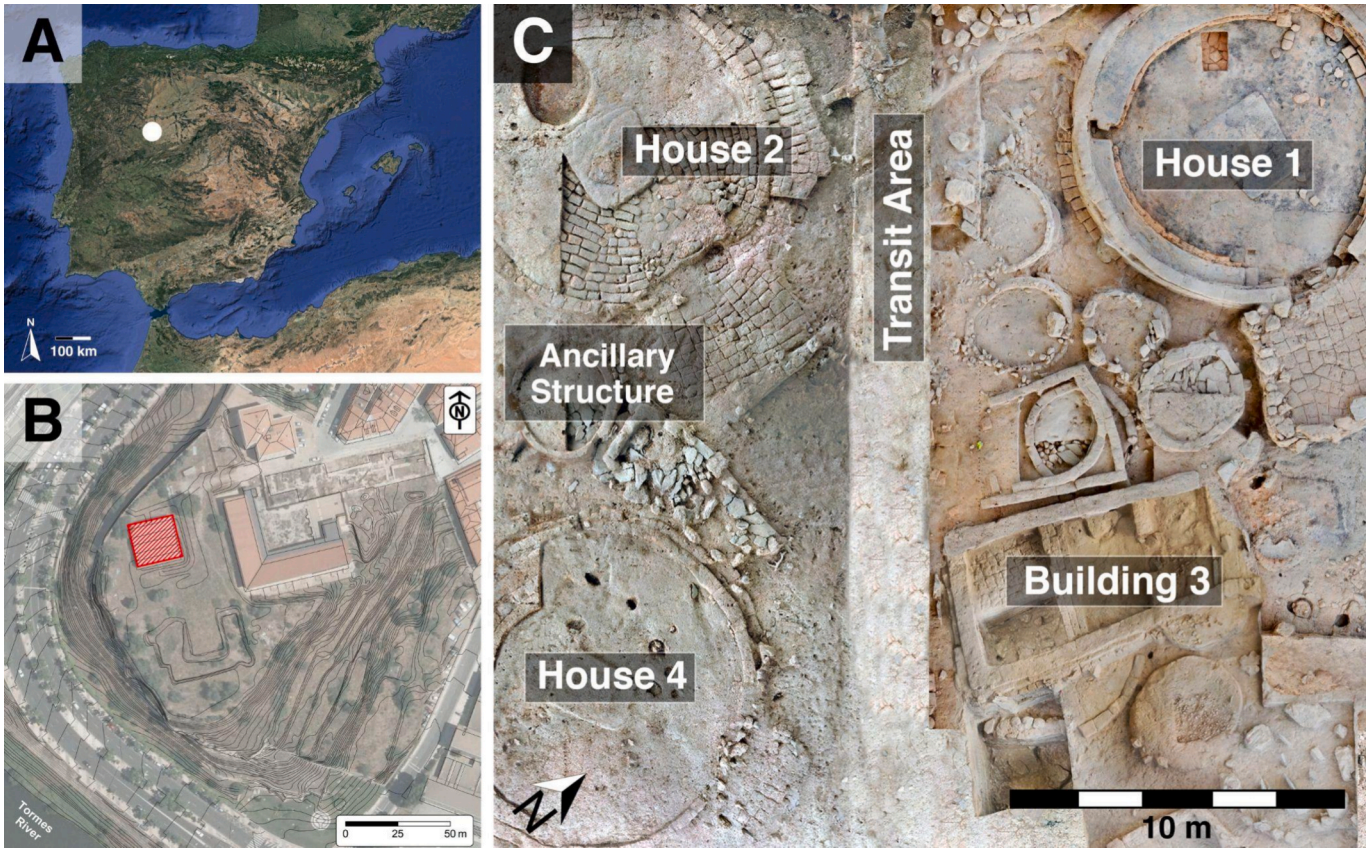

Fig. 1. A) Geographic location of Cerro de San Vicente on the Central Iberian Plateau. **B)** Aerial view of the site, located near the Tormes River, with the area targeted in this study highlighted in red. **C)** Plan view of the 400 m^2 sector excavated between 2006 and 2022, showing the remains of earthen dwellings excavated to date, including roundhouses, rectangular buildings, and smaller ancillary structures (Photogrammetry by A. Martín Esquivel and L. Chapon). (For interpretation of the references to color in this figure legend, the reader is referred to the web version of this article.)

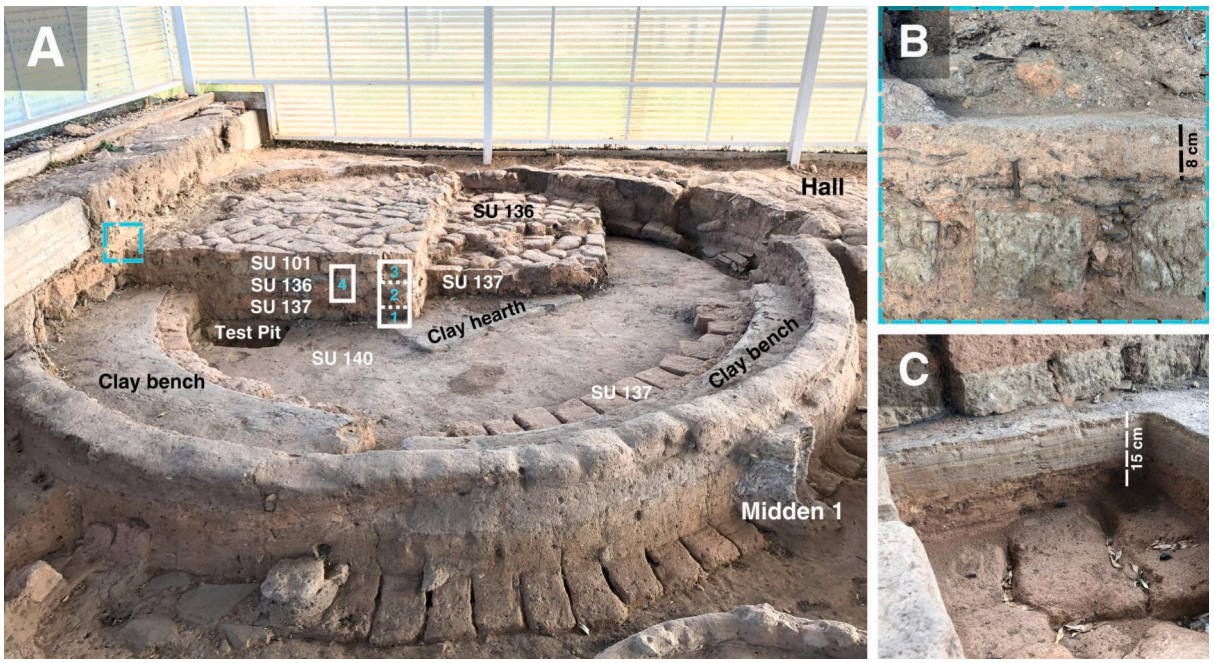

Fig. 2. **A)** Field photograph of House 1, showing key spatial and stratigraphic details. The white rectangles mark the locations where micromorphology blocks were sampled for this study, with their respective numbers labeled in light blue. Both the stratigraphic sequence from the test pit and the outer Midden 1 have been previously investigated through microstratigraphic geoarchaeological analysis (Tomé et al., 2024a; 2024b). **B)** Compact, 8 cm-thick silty-clayey deposit located directly above the upper row of the last mudbrick layer from House 1. **C)** Close-up view of the test pit sequence. Note the mudbrick layer at the bottom, followed by two major stratigraphic units separated by a sharp contact. The lower deposit consists of a compact, massive reddish silty-clayey layer with subrounded and sub-angular coarse sand and gravel-sized slate and sandstone fragments. The upper deposit is a massive, compact greyish silty-clayey unit with a bedded, micro-laminated structure composed of multiple earthen floors and floor preparation layers (Tomé et al. 2024a). (For interpretation of the references to color in this figure legend, the reader is referred to the web version of this article.)

on the preserved walls was subject to intense rubefaction—its appearance closely resembled that of fired ceramic—and that the silica in the clay melted to form what is known in archaeological literature as 'ash-slag' (Blanco-González et al. 2022). All these lines of evidence, along with the fact that the conflagration layer was solely detected inside House 1 and not outside or in any of its adjacent areas—including the outer part of the preserved walls—led researchers to propose that the dwelling underwent intentional firing, actually acting as a big oven (Blanco-González et al. 2022).

On top of the combustion layer there are three horizontally arranged layers of mudbricks, each separated by thin (1< cm) lenses of ashy sediment containing abundant charred plant remains (Fig. 2**A**, Fig. 3**C** and **D**). These mudbricks are unevenly burnt—often with only one of their faces featuring greater thermal alteration—, displaying a range of colours from pale yellow to dark reddish-brown, and some bear traces of cemented ash on their surfaces. They are laid in an interlocking horizontal pattern, with their faces aligned roughly parallel and placed side by side to form a continuous surface. Fragments of slate, pottery, and clayey mixtures were observed filling the gaps between the bricks (Fig. 3**D**). Preliminary interpretations based on the above evidence suggest that these layered mudbricks were taken from the dwelling's walls after the firing event and subsequently used to fill its interior (Blanco-González et al. 2022).

The reasons for this practice are unclear, but Blanco-González et al. (2022) suggested it might have helped start a new construction phase. The field data provide significant support for this possibility. First, an 8 cm-thick clay deposit—interpreted in the field as a potential clay pavement or floor—was excavated above the mudbrick infill within House 1 (Fig. 2**B**). Second, a test pit within House 1 revealed a succession of occupation floors and floor preparation layers, underlain by a mudbrick basement (Fig. 2**C**) (Tomé et al. 2024a). Third, a new entrance hall for House 1 was constructed atop a midden deposit, reaching the same elevation as the uppermost mudbrick layer of the house (Fig. 4**A** and Fig. 4**B**). Interestingly, other dwellings at CSV—albeit only partially excavated—exhibit a similar stratigraphy, with mudbrick layers intercalated with clay floors (Fig. 4**C**). Moreover, similar features have been documented in other villages from the same chronological and geographical context (e.g., Palol and Wattenberg 1974; Delibes de Castro et al. 1995). Thus, it is plausible that these characteristics reflect a widespread building tradition among Early Iron Age villages in the Duero valley region.

However, several questions remain unanswered and require further investigation. To better understand the burning of House 1, it is crucial to determine whether the fire and the subsequent mudbrick infilling are directly related. This connection would only be plausible if the two events occurred within a short time frame, making it essential to establish their temporal relationship. Second, what do the mudbrick layers—and the interstitial sediment between them—represent? Did the sediment accumulate gradually, indicating occupation periods between each mudbrick layer with distinct activities performed on top? Or does it represent a pavement or a single, discrete depositional event? Furthermore, were the mudbricks used to fill the house gathered from its original walls? If so, were they still part of the wall when the fire occurred? Finally, does this phenomenon respond to a specific choice or to a culturally embedded building tradition? If so, what are its defining characteristics?

In this study, we aim to address these questions by focusing on the sequence that includes the combustion deposit and the overlying mudbrick layers of House 1 through the combined application of high-resolution geoarchaeological techniques, including soil micromorphology—with charcoal analysis on thin sections—, magnetic properties analyses, X-ray diffraction (XRD), X-ray fluorescence (XRF), and GIS-based morphological and spatial analyses. This integrated approach allows for the reconstruction of the formation processes associated with the burning of House 1 and its subsequent stratigraphic sequence, the assessment of mineralogical and chemical transformations

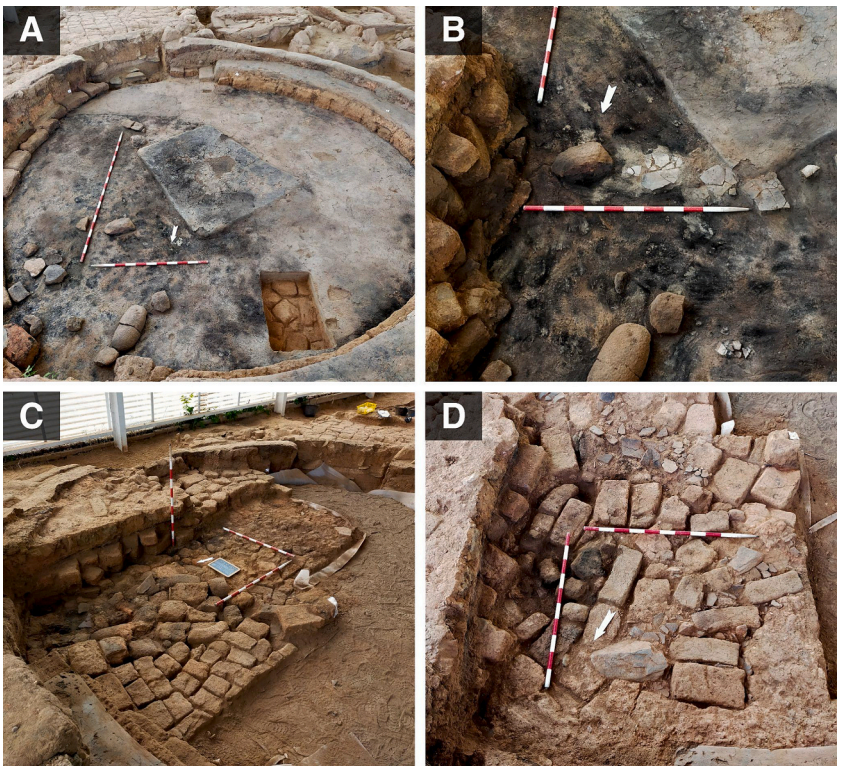

Fig. 3. Photographs documenting the excavation of House 1 during the 2021 field season. **A)** Field view of SU 140, a layer consisting of wood ash and charred plant material. **B)** Close-up view of SU 140. Note the presence of fissured pottery and stone quern fragments, placed near the central clay hearth. **C)** Field view of the excavation of SU 137, characterized by abundant mudbrick of various sizes, colors, and charring states. Above SU 137, SUs 136 and 101, which are also part of the mudbrick infilling, are represented in the stratigraphic profile. **D)** Detailed view of SU 137, showing slate and fissured pottery fragments interspersed among the mudbricks.

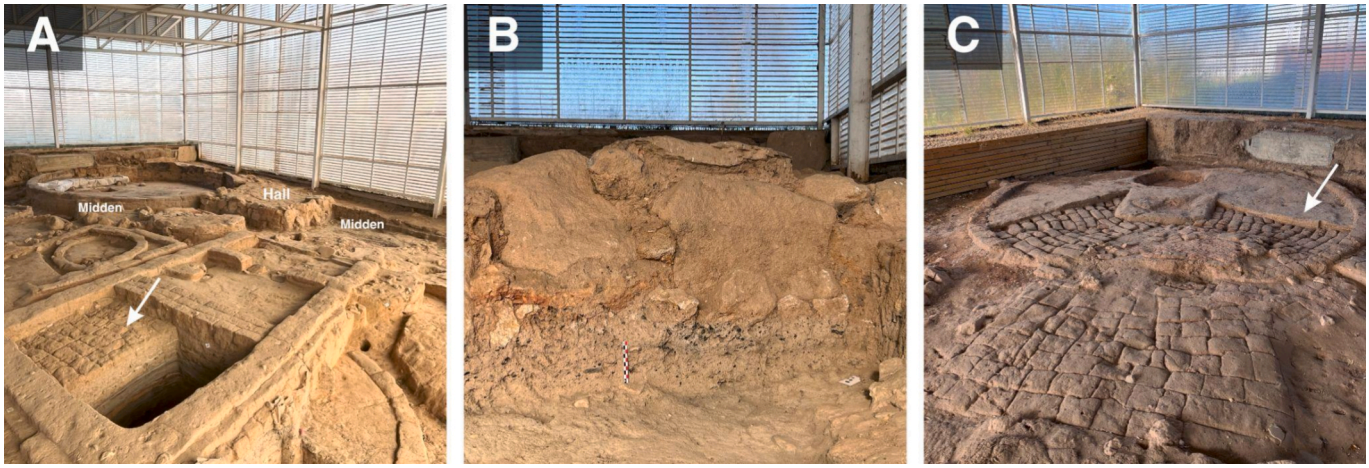

Fig. 4. **A)** View of Building 3 (foreground) with House 1 in the background. House 1 displays an elevated mudbrick entrance hall. To the left, the profile of the midden deposit located outside House 1 documented by Tomé et al. (2024b) is visible. Note that Building 3 also displays a mudbrick layer (white arrow). **B)** Close-up view of the stratigraphic profile underneath the hall of House 1. The lowest 15 cm of the sequence consists of a compact, silty ashy deposit with abundant charcoal fragments, typical of midden deposits at CSV. This is overlain by a thin silty-clayey reddish layer, along with sandstone and slate fragments. **C)** House 2. A mudbrick layer is visible inside the structure. Above it, lies a ~10 cm-thick microstratified deposit (white arrow) comprising silty-clayey floors and floor preparation layers, as documented by Tomé et al. (2024a).

in earth-based construction materials caused by fire, and the exploration of the potential origins of the mudbricks used to infill the dwelling. This study builds upon previous geoarchaeological research conducted at CSV (García-Redondo et al. 2021; Tomé et al. 2024a, b), aiming to shed light on the broader cultural implications of House 1′s final arrangement, the social and communal practices involved, and the overall dynamics of daily life within the village.

2. Materials and methods

2.1. Site background: Cerro de San Vicente

CSV is an Early Iron Age (*ca.* 900–400 BCE) settlement that lies on a flat-topped sandstone hill at 805 masl, situated on the right bank of the Tormes River. It is positioned on the westernmost edge of the Duero

Basin, intersecting with the Eastern boundary of the Central Iberian Zone within the Hesperian Massif (Julivert et al. 1972). The site was strategically located at the crossroads of various long-distance trade routes (e.g., Vía de la Plata), facilitating its connectivity with the Mediterranean (Chapon et al. 2024).

Discovered in 1951, the site has been the subject of intermittent excavations since 1990, revealing a settlement spanning 1.3 ha (Blanco-González et al. 2017, Blanco-González et al., 2024; Macarro Alcalde and Alario García 2012). Between 2006 and 2022, investigations uncovered a 600 m^2 area corresponding to the village's latest documented phase, archaeomagnetically dated between 654 and 575 BCE (García-Redondo et al. 2021). This excavation sector included several exceptionally well-preserved earthen dwellings, with mudbrick walls and clay floors: five roundhouses, two rectangular buildings, and thirteen smaller circular structures interpreted as the foundations of above-ground silos (Blanco-González et al. 2017). The dwellings contained very few archaeological remains, suggesting they were carefully emptied prior to abandonment (Blanco-González et al. 2022). Thick, ashy deposits—interpreted as middens and transit areas within the village—were documented interspersed among the dwellings. These archaeologically rich layers contained abundant potsherds, faunal remains, and charcoal (Blanco-González et al. 2022). Additionally, a notable collection of Mediterranean imported artifacts have been documented in the context of House 1 (Blanco-González et al., 2022, 2023a,b; Chapon et al., 2024).

The sequence excavated to date shows a dynamic of continuous superimposition of architectural structures and refuse deposits, leading to the accumulation of successive occupational phases, a pattern that has been documented across similar sites in the Duero Basin (Delibes de Castro et al. 1995). This excavated area of the site has been interpreted as part of a multi-family courtyard around a central open area, shared by an extended household group (Blanco-González et al. 2022, 2023a).

High-resolution geoarchaeological analyses have been previously conducted in this sector of CSV, focusing both on the dwelling floors (Tomé et al. 2024a) and the midden deposits (Tomé et al. 2024b), employing a combination of techniques: soil micromorphology, sedimentary lipid biomarker analyses, XRD, XRF, and magnetic properties analyses. Inside the buildings, complex sequences of recurrent cycles of floor use, refurbishment, and decay were documented. Micromorphological observations revealed that inner floors were carefully maintained over time, likely through sweeping and/or the use of mats for protection, resulting in a scarcity of anthropogenic components. Furthermore, the construction materials documented in the targeted sequences were microscopically, mineralogically and geochemically characterized. In contrast, the midden deposits were interpreted as the by-product of multiple hearth rake-out events, as well as maintenance and construction activities performed within the village. These studies provided a comprehensive understanding of the interplay between communal maintenance practices, construction techniques, and refuse management within the settlement, shedding light on the broader social and functional dynamics of daily life at CSV.

2.2. Archaeological soil micromorphology

Four intact, oriented sediment blocks were collected from the upper sequence of House 1 (Fig. 2**A**), including field stratigraphic units (SUs) 140, 137, 136 and 101. Blocks 1, 2, and 3 were processed at Wagner Petrographic (Utah, USA) and divided into 5 thin sections measuring 5 cm × 3 cm × 30 μm. Block 4 underwent processing at the Spanish National Research Center for Human Evolution-CENIEH (Burgos, Spain), where it was transformed into two thin sections measuring 9 cm × 6 cm × 30 μm. An additional micromorphology sample was processed from a control mudbrick collected inside House 1, placed right on top of the ash layer associated with the burning event, which resulted into two thin sections measuring 5 cm × 3 cm × 30 μm processed at the Nucleus-Rock Preparation Laboratory of the University of Salamanca (Salamanca, Spain) (see supplementary material S1). Micromorphological analyses were conducted using two petrographic microscopes available at the MICROLab, in the Interdisciplinary Center for Archaeology and the Evolution of Human Behavior (ICArEHB, Universidade do Algarve, Faro, Portugal): Nikon LV100ND and Nikon Eclipse SMZ25. Nikon DS-Ri2 and Fi3 binocular cameras were employed for capturing microphotographs.

Thin section description and interpretation adhered to the standard guidelines provided by Stoops (2003) and Nicosia and Stoops (2017). We applied the concept of microfacies unit (MFU) with the aims of identifying, differentiating and characterizing depositional events. The microfacies type (MFT) approach was applied to categorize microfacies exhibiting similar and recurrent micromorphological characteristics (Courty 2001; Goldberg et al. 2009), as it has already been successfully applied in previous micromorphological studies at CSV (Tomé et al. 2024a, b) as part of an ongoing extensive geoarchaeological study of the site.

2.2.1. Charcoal analysis

Charcoal analysis on thin sections involved taxonomic identification based on the cross sections of wood fragments, compared with wood anatomy atlases (Schweingruber 1990; Äkkemik and Yaman 2012). Due to the limitations of thin section observation, diagnostic features could not be analyzed in all three anatomical sections for each charcoal fragment, reducing the number of potentially identifiable remains. All identified fragments were measured along their largest dimension and classified according to the categories proposed by Marquer and Otto (2020). In addition to taxonomic identification, taphonomic aspects related to the presence of degraded wood were recorded in parallel (Martín-Seijo 2024).

2.3. Magnetic properties analyses

The magnetic properties of representative samples of different types of mudbrick from House 1—including the mudbrick infilling—, as well as from the wall, the central fireplace and its surrounding floor have been analyzed. Previously, some samples from the central fireplace and the floor around it were already demagnetized for archaeomagnetic dating purposes (García-Redondo et al. 2021). However, additional samples from new areas have been included here to evaluate whether they were burnt and, if so, to estimate their heating temperatures. The Koenigsberger ratio [(Q_n = NRM / (χ*H)] (cf. Stacey, 1967) has been measured to the entire collection. This ratio relates the remanent and the induced magnetization, being χ the magnetic susceptibility and H the intensity of the local Earth's magnetic field. The natural remanent magnetization (NRM) was measured with a 2G cryogenic magnetometer and the magnetic susceptibility with a KLY-4 kappabridge (AGICO). The Q_n ratio is widely used in archaeomagnetism and yields a quick estimate of the efficiency of the magnetization mechanism. In the case of potentially burnt materials, it is a useful parameter to assess whether they carry a thermoremanence (TRM). The Q_n ratio was measured in 97 samples from the different mentioned areas. The samples were meticulously subsampled from intact, sediment blocks adjacent to micromorphology blocks 1, 2 and 3, guided by changes in sediment texture, composition and colour. Additionally, samples from the wall, as well as fragments of mudbricks from inside House 1 which had been previously excavated were included. The latter were distinguished by their colors (brown, green, pink, and red), with varying degrees of burning.

Additionally, representative samples of all mudbricks were analyzed with a variable magnetic field translation balance (MM_VFTB). These analyses included the progressive isothermal remanent magnetization (IRM) acquisition curves, hysteresis cycles (±1T), backfield curves and thermomagnetic curves (magnetization *vs* temperature) in air up to a maximum temperature of 700 °C. After correcting the hysteresis cycles for their dia/paramagnetic fraction, the saturation magnetization (Ms), the remanent saturation magnetization (Mrs) and the coercive force (Bc) were determined using the Rock_Mag Analyzer software (Leonhardt 2006). The remanent coercive force (Bcr) was calculated separately

from the backfield coercivity curves. These parameters are related to the type of ferromagnetic mineral, its concentration and domain state (granulometry). The S-ratio was also calculated following Bloemendal et al. (1992) varying between 1 and 0. It provides an estimate of the relative contribution to the remanent magnetization of ferrimagnetic minerals (e.g., magnetite and/or maghemite) *vs* antiferromagnetic minerals (e.g., haematite and/or goethite). All the magnetic analyses were carried out at the Laboratory of Paleomagnetism of University of Burgos, Spain.

2.4. Mineralogy (XRD) and elemental geochemistry (XRF)

X-ray Diffraction (XRD) and X-ray Fluorescence (XRF) semi-quantitative analyses were performed on 16 bulk sediment samples at the I + D + i Scientific-Technological Centre of the University of Burgos (Spain). First, 10 sediment samples were meticulously subsampled from intact, oriented sediment blocks adjacent to micromorphology blocks 1, 2 and 3, guided by changes in sediment texture, composition and colour. Other samples (6) were directly collected from mudbricks within the infill.

For mineralogical analysis (XRD), samples were carefully dry-cleaned and powdered using an agate mortar. Semiquantitative (% weight) mineralogical analysis was conducted using a Bruker D8 Advance diffractometer. Diffractogram interpretation and mineral identification were carried out with the *DRIFACplus basic EVA* software, with a detection limit set at 1 % wt.

For elemental geochemical analysis (XRF), sediment samples were powdered, homogenized, and mixed with flux (Lithium Metaborate/Tetraborate, 0.5 % KBr), then transformed into beads using an Equilab F1 Induction fluxer. Semiquantitative (% weight) analysis of the samples was conducted with a Thermo ARL ADVAT XP Sequential XRF spectrometer. The XRF equipment had a detection limit of 0.01 % wt, but only data for major elements above 1 % wt were considered. Data interpretation was performed using WinXRF.ADVANT 3.2.1 and UNIQUANT v.5.47 software packages.

Additionally, the organic carbon present in the samples was measured through thermal oxidation method or Loss on Ignition (LOI). 0.7–0.8 g of milled and homogenised sample were heated to 110 °C for 14 h inside the muffle (Heron HD-230 PAD) and then to 550° for 5 h. The weight of the samples was measured after each heating using an analytical balance and the lost organic C calculated according to Santisteban et al. (2004).

A Principal Component Analysis (PCA) was performed on the geochemical and magnetic properties data, including previous mudbrick data (6 mudbrick samples) published by Tomé et al. (2024a). The geochemical data was normalized to Z-scores to avoid scaling effects and to obtain average-centred distributions. PCA was performed with SPSS 28.0 software to reduce the number of variables to a set of Principal Components (PCs), representative of groups of features following similar trends. Rotated (Varimax) and non-rotated solutions were evaluated, and the most suitable one to the geochemical data variance was selected (rotated: varimax).

2.5. GIS-based morphological and spatial analyses of mudbricks

Mudbricks from SUs 101 (n = 110) and 137 (n = 126) were digitized as 2D polygons in ArcGIS Pro v.3.1. We calculated the area of each mudbrick and applied the Jenks classification method, which optimizes the grouping by minimizing internal variance within each category while maximizing differences between them, relying on the inherent distribution of the dataset (Jenks, 1967; Sánchez-Romero et al., 2021; applications to Iron Age: Diwan, 2020). This step aimed to avoid including fragments or excessively small mudbricks that may represent broken pieces, which could introduce noise into the sample.

Furthermore, we performed an Optimized Hotspot Analysis using the area as the *input* variable to explore their spatial distribution and assess potential taphonomic patterns (Lee and Wong, 2001; Sánchez-Romero et al., 2021; Lin and Chen, 2023; applications to Iron Age: Wright et al., 2020). Subsequently, we selected a representative sample of 20 mudbricks—10 from SU 137 and 10 from SU 101—distributed across different areas of House 1 based on the Hotspot Analysis results.

To explore the origin of the mudbricks and their relationship with the house wall, we calculated the osculatrix circumference for the wall and for each selected mudbrick, using the longest side of each as a basis (Tabachnikov and Timorin, 2013). From these osculatrix circumferences, we derived their area, perimeter, and diameter. As a hypothesis, larger osculatrix circumferences would be associated with straighter mudbricks, while smaller ones would correspond to more curved ones. Finally, the areas, perimeters, and diameters of the osculatrix circumferences were statistically analysed through Principal Component Analysis (PCA) using Python 3.12 and Spyder 6.0.3.

3. Results

3.1. Archaeological soil micromorphology

3.1.1. Lithology, microstructure and porosity

The samples display a consistent lithological composition, primarily consisting of terrigenous, siliciclastic sediments with abundant angular and subangular quartz grains, ranging in size from fine sand to gravel, alongside angular fine sand-sized mica-group minerals. Gravel to sand-sized angular and subangular slate and quartzite are present in smaller quantities.

Massive microstructures are the most prevalent and are observed consistently throughout the sequence. Complex microstructures are also present, displaying a combination of massive with spongy, platy, or intergrain microaggregate, particularly at the bottom and top of the sequence. Through all the samples, a porphyric c/f related distribution is predominantly detected. Vughs and vesicles are the most abundant porosity types, followed by planes, moldic, and complex packing voids. Channels and chambers have also been identified, though in lower proportions. Bioturbation features are minimally present and primarily consist of channels, moderately developed calcium carbonate hypocoatings on voids, and granotubules.

A detailed description of the micromorphological features present in each sample, as well as microphotographs displaying representative microstructures, are provided in supplementary material (S2, S3).

3.1.2. Anthropogenic components

Anthropogenic components are present throughout the sequence and are particularly abundant both in the deposit between the charred clay floor and the lowermost unit, and in the layers between mudbricks. These mainly consist of calcitic wood ash, charcoal, coarse silt to fine sand-sized charred plant matter, and earth-based construction material fragments (displayed as anorthic, disorthic and orthic nodules). A more detailed description of these components is provided in Table 1 and Fig. 5. For the specific location of the components within each sample, refer to Table 2 and supplementary material (S2).

3.1.3. Microfacies units (MFU) and microfacies types (MFT)

A total of 9 microfacies units (MFU) were identified throughout the sequence. These MFUs are correlated with 16 bulk sediment samples on which XRD, XRF and magnetic properties analyses were conducted (see supplementary material S2). The distribution of each MFU across the samples and their main micromorphological features are shown in Fig. 6 and Table 2. These MFU have been categorized into 3 microfacies types (MFT) (Fig. 7, Table 3), which can be added to the MFT documented by Tomé et al. (2024a, b) at CSV (see supplementary material S4), bringing the total number of MFT documented at the site so far to 13. As Microfacies Types 1 to 11 have already been published, the new MFTs presented here are labeled as MFT 12 and MFT 13. Additionally, a new variation of a previously documented microfacies (MFT 5a) is

Table 1
Description of the main components identified in the micromorphological samples. Microphotographs of each component are presented in Fig. 4. For detailed information on the specific location and abundance of the components in each sample, refer to Table 2 and supplementary material (S2).

Component	Description	Significance
Calcitic wood ash	Very abundant in the sediment layer between the clay floor and the lowermost mudbrick row, and moderately present between mudbrick rows Displayed either 1) intact, with a spongy/platy microstructure, or 2) reworked, as rounded and subrounded sand-sized aggregates Usually mixed with charcoal, sand-sized charred plant matter and earth-based construction materials fragments Calcium oxalate crystals	High-temperature wood burning activity
Charcoal	Very abundant in the sediment layer between the clay floor and the lowermost mudbrick row, abundant between mudbrick rows Subangular and subrounded Sand to gravel-sized Mostly well-preserved, with intact inner cell structure Usually mixed with calcitic wood ash and sand-sized charred plant matter	Wood burning activity
Charred plant matter	Very abundant in the sediment layer between the clay floor and the lowermost mudbrick row, abundant between mudbrick rows Subrounded and rounded Sometimes fine and elongated Fine sand-sized Usually mixed with calcitic wood ash and charcoal	Plant burning activity
Earth-based construction materials	Present throughout the whole sequence Sand to gravel-sized anorthic, orthic and/or disorthic nodules Usually displayed as: 1) yellow clay nodules with iron staining, containing coated angular quartz sand (~60 %), 2) light yellow/brown grano-striated clay nodules with quartz and slate sand, and fine sand-sized mica-group minerals	Suggests discard and/or decay of earth-based construction materials

introduced here as MFT 5b.

The mudbrick layers contain both unburnt (MFT 5a) and burnt (MFT 5b) mudbrick, along with deposits of compact, massive sandy-clayey earth-based construction materials, interpreted as mortar (MFT 13). Between mudbricks, layers of charred plant material, reworked wood ash and disintegrated and fragmented earth-based construction materials (MFT 12a) were observed. In contrast, the sediment between the charred clay floor and the lowermost mudbrick layer is dominated by a massive calcitic-crystallitic wood ash deposit (MFT 12b).

3.1.4. Charcoal analysis

A total of 21 charcoal fragments were taxonomically identified on thin sections. The identified charcoal pieces range in size from 0.5 mm to 8 mm (supplementary material S4). Overall, 5 taxa were identified: evergreen and deciduous *Quercus*, *Quercus* sp., *Pinus* sp. and dicot (Fig. 8). The measurements of the longest side size of each charcoal fragment and their correlation with MFU are presented in supplementary material S5. The charcoal is unevenly distributed across the different MFUs, with a concentration in the lower part of the sequence (MFU 1a), where the largest charcoal fragments (8–3 mm) were also recorded. The presence of decayed wood prior to charring was identified in MFU 1a (small twig of *Pinus* sp. with 4 preserved annual rings and two xylophagous galleries, and evergreen *Quercus* with one gallery).

3.2. Magnetic properties analyses

Magnetic properties results are illustrated in Fig. 9, supplementary material S6 and S6. The values of the Q_n ratio (Fig. 9**A**) range from 0.72 to 21.14 with clear variations between types of samples. It is generally assumed that values above unity are likely to carry a TRM (Stacey 1967), although the higher the values, the better. The samples from the central fireplace (n = 30) range from 4.3 to 13.59. The mudbrick wall samples (n = 18) were analyzed differentiating between the reddish external part (Q_n ratio values between 6.35 and 15.65) and the darker internal part (Q_n ratios between 13.68 and 20.82). The samples of the floor are composed of 7 hand blocks (38 specimens) collected around the central fireplace and range from 1.0 to 11.51. Finally, the mudbrick sample set (n = 14), denoted as triangles in Fig. 9, exhibits Q_n values from 0.72 to 21.14. The orthogonal NRM thermal demagnetization is shown in supplementary material S7, with plots of two floor samples around the central fireplace and another one from the central hearth. The floor samples exhibit a paleomagnetic component or vector (blue line) with maximum unblocking temperatures (max T_{UB}) of 450–500 °C, which would correspond to the last recorded heating of these materials (Supplementary material, S7A-B). In contrast, the samples from the central fireplace are much more magnetic and exhibit a single vector with max T_{UB} of 575 °C (Supplementary material, S6C).

Thermomagnetic curves and their degree of reversibility were analyzed to explore paleotemperatures. Fig. 9**B–G** illustrates representative examples of the materials studied. The control mudbrick sample (Supplementary material, S1), both its red outermost part (Fig. 9**B**) and its dark inner part (Fig. 9**C**) are highly magnetic and dominated by magnetite (Curie temperature or T_C = 580 °C). They are fully reversible up to 700 °C. This indicates that they were heated at least to that temperature. Their mean Qn ratios are also very high (>10), which supports this interpretation (Fig. 9**A**). Fig. 9**D** and Fig. 9**E** illustrate thermomagnetic curves of two floor samples heated in the lab to 600 °C and 500 °C, respectively. The sample heated to 600 °C is irreversible, while the one heated to 500 °C is fully reversible. This indicates that this floor sample (CSV9) was archaeologically heated between 500 and 600 °C. Fig. 9**F** shows a thermomagnetic curve of a hematite-dominated mudbrick (T_C = 675 °C), while Fig. 9**E** represents a red mudbrick dominated by hematite and maghemite, both sampled from House 1 infilling. In both cases the curves are irreversible but their high Q_n values and other mineral concentration-dependent parameters such as M_s, M_{rs} or SIRM (supplementary material S6) indicate that they were heated in the past. The red mudbrick shown in Fig. 8**G** displays a Q_n value of 21.14, indicating that it carries a stable TRM as it was heated at high temperature, likely >600–700 °C.

Field observations noted color variations in mudbrick samples, classified as “possibly burnt” or “possibly unburnt” (supplementary material S6). The “possibly unburnt” samples exhibit the lowest Q_n ratio values, such as the “unburnt red” (RJNQ) and “unburnt green” (VNQ) mudbricks, both with Q_n ratio values <1. Their Q_n values are not very different from those of “brown” (MR) and “unburnt pink” (RNQ) mudbricks, both between 1 and 2 (Fig. 9**A**, supplementary material S6), suggesting that the limit of 1 should be considered as an empirical approximation. It cannot be totally ruled out that the mudbrick samples with the lowest Q_n values correspond to the internal or less burnt part of them. Q_n values above 3 or 4 may well be carriers of a TRM and therefore heated to high temperature. The “possibly burnt” samples, such as the “burnt green” (VQ) and “burnt red” (RJQ) mudbricks, show higher Q_n

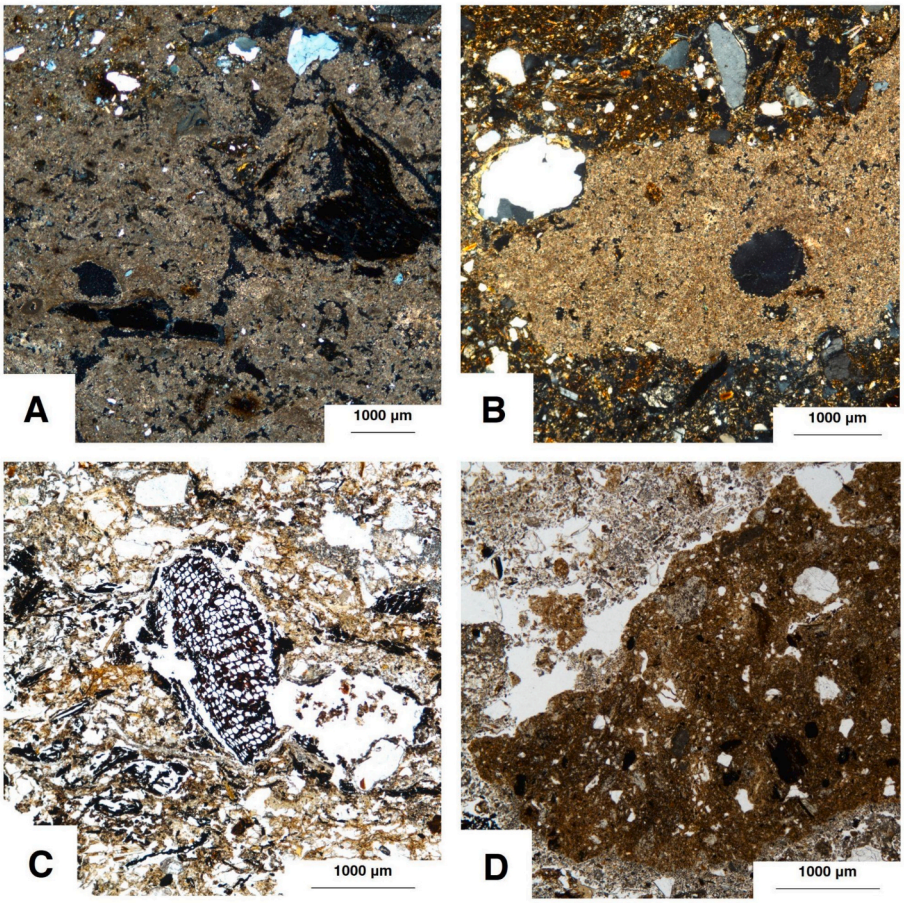

Fig. 5. Microphotographs of the predominant microscopic anthropogenic components identified in House 1. Detailed descriptions of each component are presented in Table 2. **A)** XPL. Intact, massive calcitic-crystallitic wood ash, with few charcoal and sand-sized earth-based construction material inclusions. Exclusively documented in the deposit between the charred clay floor and the lowermost mudbrick layer. **B)** XPL. Subrounded calcitic-crystallitic wood ash aggregate, interspersed among mudbricks layers. **C)** PPL. Charcoal. Very abundant between mudbrick layers and in the deposit between the clay floor and the lowermost mudbrick row. It occurs in various sizes, typically with subrounded, subangular or elongated morphologies. While often well preserved, some fragments show evidence of insect bioturbation, as illustrated in the microphotograph. **D)** PPL. Earth-based construction material fragments. Very abundant throughout the whole sequence. As shown in the microphotographs, these fragments typically appear as anorthic brown silty-clayey nodules with sharp boundaries, containing quartz, slate sand, and mica-group minerals.

values, of 6.20 and 21.14, respectively (Fig. 9**G**, supplementary material S6), indicative that they were well-heated in the past. Such a visual description made in the field agrees quite well with the magnetic results. Further evidence is that those samples originally described as "possibly burnt" also show Ms, Mrs or SIRM values around one order of magnitude higher than that of their unburnt counterparts (supplementary material S6).

Many mudbricks have significantly low S-ratio values but high Q_n ratio values. For example, this is the case of sample CSV21-2-1b (middle mudbrick layer), with an S-ratio of 0.23 and a Q_n ratio of 14.93 (supplementary material S6). This indicates that this sample was heated at high temperature (high Qn ratio) and generated hematite (low S-ratio). With the exceptions already mentioned and within their variability, something similar happens with the other mudbricks studied.

3.3. Mineralogy (XRD) and elemental geochemistry (XRF)

All the samples showed similar mineralogical (XRD) and geochemical (XRF) compositions. Mineralogically, quartz, clay minerals, and feldspars are the most abundant minerals in the samples, corresponding to mud (clay minerals) and sand to pebble-sized grains (quartz and feldspars) observed in the samples (Fig. 10**A**, supplementary material S8). Quartz, the most abundant mineral in all the samples, varies from 87.8 % to 45.4 %, the clay minerals from 40.2 % to 4.51 % and the feldspars are also abundant, from 43 % to 4 %. Calcium carbonate content (calcite) is less abundant but significant, ranging from 0 % to 5.5 %.

On the other hand, the elemental geochemical composition analysis (XRF) also showed a similar composition for all the samples, with SiO_2 as the predominant compound (between 77 % and 61 %), followed by Al_2O_3 (between 21 % and 13.8 %) and Fe_2O_3 (between 8 % and 2 %). CaO, K_2O, Na_2O, MgO, TiO_2, Br, P_2O_5, SO_3 were also documented, but in lower proportions (less than 3 %) (Fig. 10**B**, supplementary material S8). The organic carbon (Corg) content of the samples is quite homogeneous varying between 7 % and 2 % (supplementary material S8).

Principal component analysis was performed on the geochemical and magnetic properties data of the samples (supplementary material S9, Fig. 10**C** and Fig. 10**D**). Overall, the variation in elemental geochemical composition of the samples is explained by four principal components (PC_1 to PC_4 in supplementary material S9 and Fig. 10), which together account for 89.1 % of the variance. PC_1 explains 30.7 % of the variance. Fe_2O_3, Al_2O_3 and TiO_2 show high positive factor loadings (>0.7). SiO_2 and MgO have high negative factor loadings. PC_2 explains 20.6 % of the variance; CaO, LOI-Corg, P_2O_5 and SO_3 have high positive loadings. PC_3 explains 19 % of the variance; magnetic properties (χ, J and Q_n) have high positive factor loadings. Finally, PC_4 explains 18.8 % of the variance; K_2O and Na_2O have high positive factor loadings, and Br and SO_3 have significant negative loadings.

Table 2
Description of the main micromorphological features recorded in each microfacies unit (MFU) and their correlation with microfacies types (MFT) and bulk sediment samples. For a more detailed description of each MFU, see supplementary material S2.

MFU	MFT	Bulk sediment sample	Micromass	Microstructure	Porosity	Lithology	Anthropogenic components
1a	12b	CSV21-3–3 CSV-21–3-4	Calcitic-crystallitic	Complex (spongy and crumb)	Vughs and vesicles (~20–25 %), complex packing voids (~10–15 %), planes (~10–15 %)	Medium-to-fine sand-sized subangular and angular quartz (~10–15 %), fine sand-sized angular mica-group minerals (~10–15 %), sand-sized subangular slate (~5–10 %), sand-sized subangular quartzite (~<5%)	Very abundant calcitic-crystallitic wood ash Very abundant charred plant matter Very abundant charcoal Abundant earth-based construction material fragments Few burnt animal bone
1b	12b	CSV21-3–3 CSV21-3–2	Calcitic-crystallitic	Complex (spongy with platy domains / crumb)	Planes (~15–20 %), vughs and vesicles (~10–15 %), complex packing voids (~5–10 %), channels (~5%)	Medium-to-fine sand-sized subangular and angular quartz (~10–15 %), fine sand-sized angular mica-group minerals (10–15 %), sand-sized subangular slate (5–10 %), sand-sized subangular quartzite (<5%)	Very abundant calcitic-crystallitic wood ash Very abundant charred plant matter Very abundant charcoal Abundant earth-based construction material fragments
2	12a	CSV21-3–1	Reddish brown, grano-striated and undifferentiated	Massive	Planes (~10–15 %), vughs and vesicles (~10–15 %), moldic voids (~10–15 %) channels (~5%)	Medium-to-fine sand-sized subangular and angular quartz (~15–20 %), sand-sized subangular slate (~5–10 %), fine sand-sized angular mica-group minerals (~15–20 %)	Very abundant earth-based construction material fragments Calcitic-crystallitic wood ash Charred plant matter Few charcoal
3	5a	CSV21-2–4 CSV21-2–3	Light brown, grano-striated	Massive	Vughs and vesicles (~10–15 %), moldic voids (~10–15 %), chambers (~5%), vertical planes (~5%)	Medium-to-fine sand-sized subangular and angular quartz (~25–30 %), fine sand-sized angular mica-group minerals (~15–20 %), sand-sized angular slate (~5–10 %), sand-sized angular quartzite (~<5%)	Few earth-based construction material fragments Few charcoal
4	5b	CSV21-2–2 CSV21-2–1	Reddish brown, grano-striated	Massive	Vughs and vesicles (~15–20 %), channels (~10–15 %), moldic voids (~10–15 %), planes (~5–10 %)	Sand-sized subangular slate (~20–25 %), fine sand-sized angular mica-group minerals (~20–25 %), medium-to-fine sand-sized subangular and angular quartz (~15–20 %)	
5	12a	CSV21-1–2	Light brown, undifferentiated and calcitic-crystallitic	Massive	Vughs (~15–20 %), chambers (~5–15 %), channels (~5%)	Fine-to-medium sand-sized subangular and angular quartz (20–25 %), fine sand-sized angular mica-group minerals (20–25 %), sand-sized subangular slate (5 %)	Very abundant calcitic-crystallitic wood ash (aggregated) Abundant charred plant matter Abundant charcoal Abundant earth-based construction material fragments
6	13	CSV21-1–2 CSV21-1–1	Dark brown, grano-striated	Massive	Vughs (~5–10 %), channels (~5–10 %), chambers (~<5%), moldic voids (~<5%)	Fine-to-medium sand-sized subangular and angular quartz (~45–50 %), medium subangular quartzite sand (~<5%), gravel-sized subangular quartzite (~<5%), medium subangular sand slate (~5–10 %), fine sand-sized angular mica-group minerals (~25–30 %)	
7a	12a	CSV21-1–1	Brown, undifferentiated, mixed with calcitic-crystallitic	Massive	Vughs (~10–15 %), channels (~5%), chambers (~5%), planes (~5%)	Fine-to-medium sand-sized subangular and angular quartz sand (~15–20 %), fine sand-sized angular mica-group minerals (~15–20 %), sand-sized subangular slate (~5%)	Very abundant calcitic-crystallitic wood ash (aggregated) Very abundant charred plant matter Very abundant charcoal Earth-based construction material fragments
7b	12a	CSV21-1–1	Brown, undifferentiated, mixed with calcitic-crystallitic	Massive	Vughs (~10–15 %), channels (~5%), chambers (~5%), planes (~5%)	Fine-to-medium sand-sized subangular and angular quartz sand (~20–25 %), fine sand-sized angular mica-group minerals (~20–25 %), sand-sized subangular slate (~5%)	Very abundant calcitic-crystallitic wood ash (aggregated) Abundant charred plant matter Abundant charcoal Abundant earth-based construction material fragments

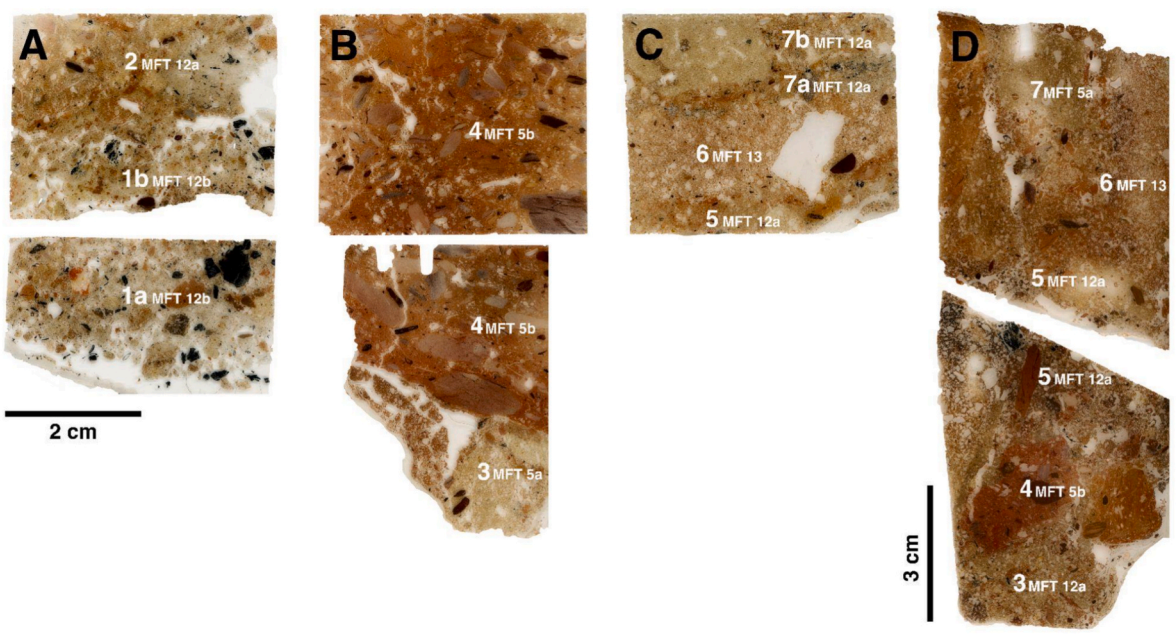

Fig. 6. Thin section scans of the House 1 sequence, showing microfacies units (MFU, white numbers) and microfacies types (MFT). **A)** Block 1 (bottom of the sequence). **B)** Block 2 (middle section of the sequence). **C)** Block 3 (upper section of the sequence). **D)** Block 4. Middle-to-upper section of the sequence.

3.4. GIS-based morphological and spatial analyses of mudbricks

The Jenks classification method produced three distinct groups of mudbricks based on their area in both SUs (Fig. 11**A** and Fig. 11**B**). Mudbricks in the smallest group ($\leq$0.05 for SU 137 and $\leq$0.03 for SU 101) were excluded from further sampling to avoid noise caused by potentially fragmented bricks.

On the other hand, Optimized Hotspot Analysis revealed significant differences between both units. In SU 137, larger mudbricks formed a hotspot in the western part of the house, while smaller ones were clustered in a coldspot in the eastern zone, separated by a central area of non-significant values (Fig. 11**C**). A similar pattern was observed in SU 101, where the southwestern part of the house exhibited a hotspot of larger mudbricks, contrasting with the northeastern zone, which showed a coldspot of smaller ones (Fig. 11**D**). Based on these results, the sampling of mudbricks prioritized well-preserved examples from Jenks groups 2 and 3, ensuring representation across different parts of the house and varying Hotspot values.

The 20 selected mudbricks displayed varying osculatrix circumference values (Fig. 11**E** and Fig. 11**F**). While some values were close to those of the wall, others deviated significantly. The scatter plot further revealed that these deviating values could be divided into two groups: those with smaller osculatrix circumferences and those with larger ones. The Principal Component Analysis supported these observations, showing a clear separation between mudbricks with wall-like values and those with divergent characteristics. Lastly, no significant differences were identified between the mudbricks of each SU.

4. Discussion

The microcontextual geoarchaeological analysis of the upper sequence of House 1—marked by a burning event and a mudbrick infill—has shed light on the processes behind its formation. Micromorphological observations reveal a thick ash layer (MFT 12b) between the charred earthen floor associated with the central clay hearth and the overlying mudbricks, which are variably burnt and unburnt (MFT 5a and 5b) and interspersed with combustion residues and earth-based construction mortar (MFT 12a, MFT 13). Charcoal analysis on thin sections identified taxa such as *Pinus* sp. and evergreen/deciduous *Quercus*. Complementary mineralogical, geochemical, and magnetic analyses provided further insights into burning temperatures and construction materials, while GIS-based spatial and morphological data helped characterize the mudbricks and assess their potential sources.

In the following sections, we discuss the evidence, integrate it with the existing geoarchaeological dataset from CSV (Tomé et al. 2024a, b), and evaluate their broader archaeological implications. This aims to advance our understanding of house burning as a cultural phenomenon during the Iberian Iron Age—and beyond.

4.1. The burning of House 1

The lowest section of the targeted sequence corresponds to field SU 140, which is macroscopically characterized by the abundant presence of combustion remains, primarily ashes and charcoal. This deposit correlates with MFU 1a and 1b (MFT 12b), which exhibit a compact calcitic-crystallitic matrix composed of wood ash (Fig. 12**A** and Fig. 12**B**), along with very abundant charcoal fragments ranging in size from silt to coarse sand, as well as earth-based construction material fragments. This ashy layer displays a platy to crumb microstructure with vughs and planes, and no evidence of ash recrystallization or aggregation. The charcoal fragments show excellent preservation, with localized features of insect bioturbation (i.e., granotubules) observed in a few fragments. Notably, some of these charcoal fragments are coarse sand-sized and exhibit a subangular to angular morphology. These features are indicative of exceptional preservation of an *in situ* combustion deposit (Mallol et al. 2013a, 2017; Mentzer 2014), suggesting limited post-depositional disturbance and rapid burial.

The thickness of the ashy deposit (~4 cm) serves as a significant indicator of the intensity of the burning event. As highlighted by Karkanas (2021), wood ash is an exceptionally porous and compressible material, with compaction reducing its thickness by approximately 90 %. In the case of House 1, the subsequent deposition of a ~60 cm-thick layered mudbricks would have further compressed the ashy layer. This indicates that the original ash deposit was substantially thicker. Additionally, based on archaeomagnetic and rock-magnetic data, the samples from the central clay hearth are highly magnetic, univectorial and with maximum unblocking temperatures of 575 °C (supplementary material, S7C), indicating that they were exposed to at least that temperature.

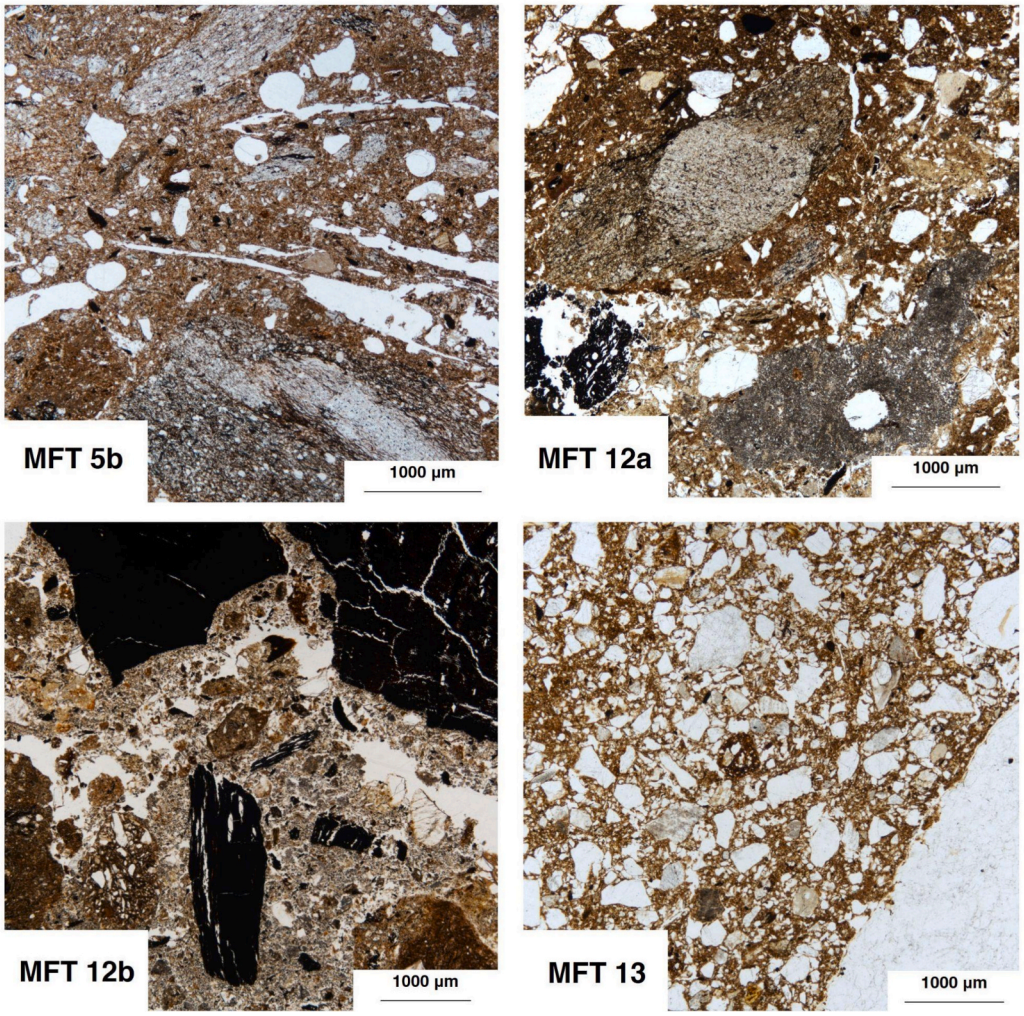

Fig. 7. Microphotographs (PPL) of the Microfacies Types (MFT) identified in the micromorphological samples. A more detailed description of each MFT is presented in Table 3. These MFT add up to the MFT documented by Tomé et al. (2024a; 2024b) in CSV (see supplementary material, S3). **MFT 5b)** Compact, massive reddish silty-clayey groundmass containing sand and gravel-sized subangular quartz and slate. Prominent features include vughs, vesicles, and moldic voids. **MFT 12a)** Massive, compact brown silty-sandy clayey groundmass, containing aggregated calcitic wood ash and abundant sand-sized subangular slate and quartz. Frequent vughs, vesicles, and packing voids. Note the presence of earth-based construction material fragments (in the top part of the microphotograph) and charcoal. **MFT 12b)** Platy, compact calcitic micromass composed of wood ash, featuring abundant charcoal, fine sand-sized charred plant matter, and fragments of earth-based construction materials. **MFT 13)** Massive, compact reddish silty-sandy clayey groundmass, with very abundant subangular and angular sand and gravel-sized quartz.

Samples from the clay floor around the fireplace show maximum unblocking temperatures between 450–500 °C (supplementary material, S7C). Thermomagnetic analysis further supports these temperature ranges, showing that the heating of floor samples did not exceed 600 °C, with reversible thermomagnetic behavior observed for samples heated to 500 °C, and irreversible behavior for those heated to higher temperatures (Fig. 9**D** and Fig. 9**E**).

Micromorphological data provides valuable insights into how the burning event affected House 1 as a whole. Earth-based construction material fragments are highly abundant in MFU 1a and 1b, appearing as sand-sized, anorthic grano-striated silty-clayey nodules with sharp, well-defined boundaries. The abundance of these fragments is further reflected in the mineralogical and geochemical composition of the associated samples, which display patterns similar to previously analysed earth-based construction materials at CSV (Tomé et al. 2024a, b), made from siliciclastic, terrigenous sediments: quartz, clay minerals and feldspar are the dominant minerals, while SiO_2 and Al_2O_3 are the most recurrent oxides. Thin section analysis revealed various types of earth-based construction materials, some of which can be associated with previously identified MFTs at CSV (supplementary material S4). The most prevalent fragments correspond to clay floor materials (MFT 2a, MFT 2b), likely from the clay floor of House 1—directly exposed to the burning event—, along with mudbrick fragments (MFT 5). Additionally, a few nodules of floor preparation fragments (MFT 1b) were also identified (Fig. 12**C**). These earth-based construction material fragments exhibit uneven reddening and darkening, suggesting they were subjected to heat and therefore impacted by the burning event. This was likely caused by fire affecting various components of the house, including the clay floor, the mudbrick walls, and the roof, which would have been directly impacted by the intense heat, leading to the fragmentation and deposition of construction material fragments along with wood ash and other combustion residues.

Charcoal taxonomic identification on thin sections also provides valuable data in the understanding of the burning event in House 1. Out of the identified taxa, *Quercus* sp. (both evergreen and deciduous) and *Pinus* sp. are the most recurrent ones. This aligns with previous anthracological analysis at House 1 SU 140 (Blanco-González et al. 2022), where *Pinus* sp. (*Pinus* tp. *pinea/pinaster*) was interpreted as a structural element in the construction, particularly in the form of beams found *in situ* at the threshold of the entrance. The presence of insect galleries and fungal hyphae in these samples indicated significant wood biodegradation, suggesting that the wood had been exposed for an

Table 3
Microfacies types (MFT) identified in the micromorphological samples and their correlation with Microfacies Units (MFU). MFTs 1b, 2a and 2b have only been documented as fragments within MFUs. Microphotographs of each MFT are displayed in Fig. 6.

Microfacies type	Description	Deposit type	Microfacies unit
1b*	Groundmass composed of light-yellow silty-sandy clay with iron staining, and coarse quartz sand (30–35 %)	Floor preparation layer	7b, 7a, 5, 3, 1a, 1b
2a*	Dark brown, homogeneous silty-sandy clayey groundmass with sand-sized quartz and slate inclusions. Abundant vughs, moldic voids and clay coatings. Compact and massive.	Earthen floor	7b, 7a, 5, 3, 2, 1b, 1a
2b*	Massive light brown silty-sandy clayey groundmass, with sand-sized quartz and slate inclusions. Abundant planes and other desiccation features. Vughy porosity.	Earthen floor	7b, 7a, 5, 3, 2, 1b, 1a
5a*	Massive, compact light yellow silty-sandy clayey groundmass (~20–25 %), with abundant angular and subangular sand-sized quartz and slate. Frequent vughs and moldic voids. Weakly developed clay coatings.	Mudbrick	3
5b	Massive, compact reddish silty-sandy clayey groundmass (~20–25 %), with abundant angular and subangular sand-sized quartz and slate. Frequent vughs and moldic voids. Weakly developed clay coatings.	Burnt mudbrick	4, Control mudbrick
12a	Massive, compact brown/reddish silty-sandy clayey groundmass (~20–30 %), with aggregated calcitic wood ash and abundant sand-sized subangular and angular quartz. Frequent vughs, vesicles and packing voids. Abundant earth-based construction material fragments, charcoal and fine sand-sized charred plant matter.	Disintegrated earth-based construction material with charred plant debris	7b, 7a, 5, 3, 2
12b	Crumb/platy calcitic-crystallitic micromass (~40–50 %), with frequent sand-sized subangular and angular quartz and slate. Very abundant charcoal, fine sand-sized charred plant matter and earth-based construction material fragments.	Destruction Layer	1b, 1a
13	Massive, compact reddish silty-sandy clayey groundmass (~15–20 %), with very abundant subangular and angular sand and gravel-sized quartz, few gravel-sized angular quartzite and subangular sand-sized slate. Few vughs and vesicles.	Construction Mortar	6

* Previously described by Tomé et al. (2024a).

extended period prior to the fire event (Blanco-González et al. 2022). Insect galleries were also detected in the microscopic charcoal fragments identified on thin sections (Fig. 8**D**). Such patterns of wood preservation and usage are typical in Iron Age contexts that have experienced fires (Martín-Seijo et al., 2020; Martín-Seijo 2024), supporting the hypothesis that the whole House 1, including its walls, roof and structural elements, was likely affected by the burning event.

The role of the roof in the burning event is particularly noteworthy. Experimental and geo-ethnoarchaeological studies (Bankoff and Winter 1979; Friede and Steel 1980; Balbo et al. 2012; Friesem et al. 2014b) suggest that, during and after a conflagration event, a roof made of perishable materials (e.g., light wood, and/or a mixture of plants and mud) would be the first structural element of the house to collapse, covering the underlying deposit with ashes and charred plant debris, as observed in House 1 SU 140. Furthermore, Gordon (1953) stated that houses with plant-based roofs would burn faster and more intensely, as the plants would rapidly fuel the fire. Previous anthracological water sieving samples from SU 140 (Blanco-González et al. 2022) identified three woody taxa, including the predominant *Pinus sp.*, as well as branches from evergreen *Quercus* and *Cistus* sp. The small caliber of these branches suggested their likely use as lighter construction materials for the roof of the house. However, we cannot rule out the possibility that *Cistus* sp. were used to start the fire as in the case of Cancho Roano (Badajoz, Spain) (Celestino Pérez et al. 2003: 339). Similarly, both evergreen and deciduous *Quercus* small charcoal fragments (1–3 mm) have been identified on thin sections (MFU 1a and 1b), alongside *Pinus* sp. fragments (ranging from 0.5 to 8 mm). Collectively, these data indicate that the roof of House 1 was likely constructed with plant perishable materials, including both heavier and lighter wood species, which played a significant role in the construction and subsequent burning of the structure. In a collapsed roof deposit, one would expect to find phytoliths; however, none were observed in the thin sections. This is likely due to the high ash content of the deposit, which is highly alkaline, and this would inhibit phytolith preservation (Cabanes, 2020). A detailed phytolith analysis of the ashy sediment is needed to confirm this preliminary interpretation.

After the collapse of the roof occurred, the floor of House 1 and the remaining combustion deposit would have been directly exposed to the exterior environment. However, as discussed above, micromorphological analysis revealed that the ashy deposit resulting from the fire remained undisturbed by external agents such as water, vegetation growth, or significant insect bioturbation. This evidence leads us to propose that the burning of House 1 and its subsequent sealing with the mudbrick infill were closely linked events that occurred in rapid succession. This rapid sealing would account for the absence of post-depositional disturbances in the ashy deposit and the clay floor beneath it (Tomé et al. 2024a). The specific processes associated with the deposition of mudbricks over the combustion layer are addressed in the following section.

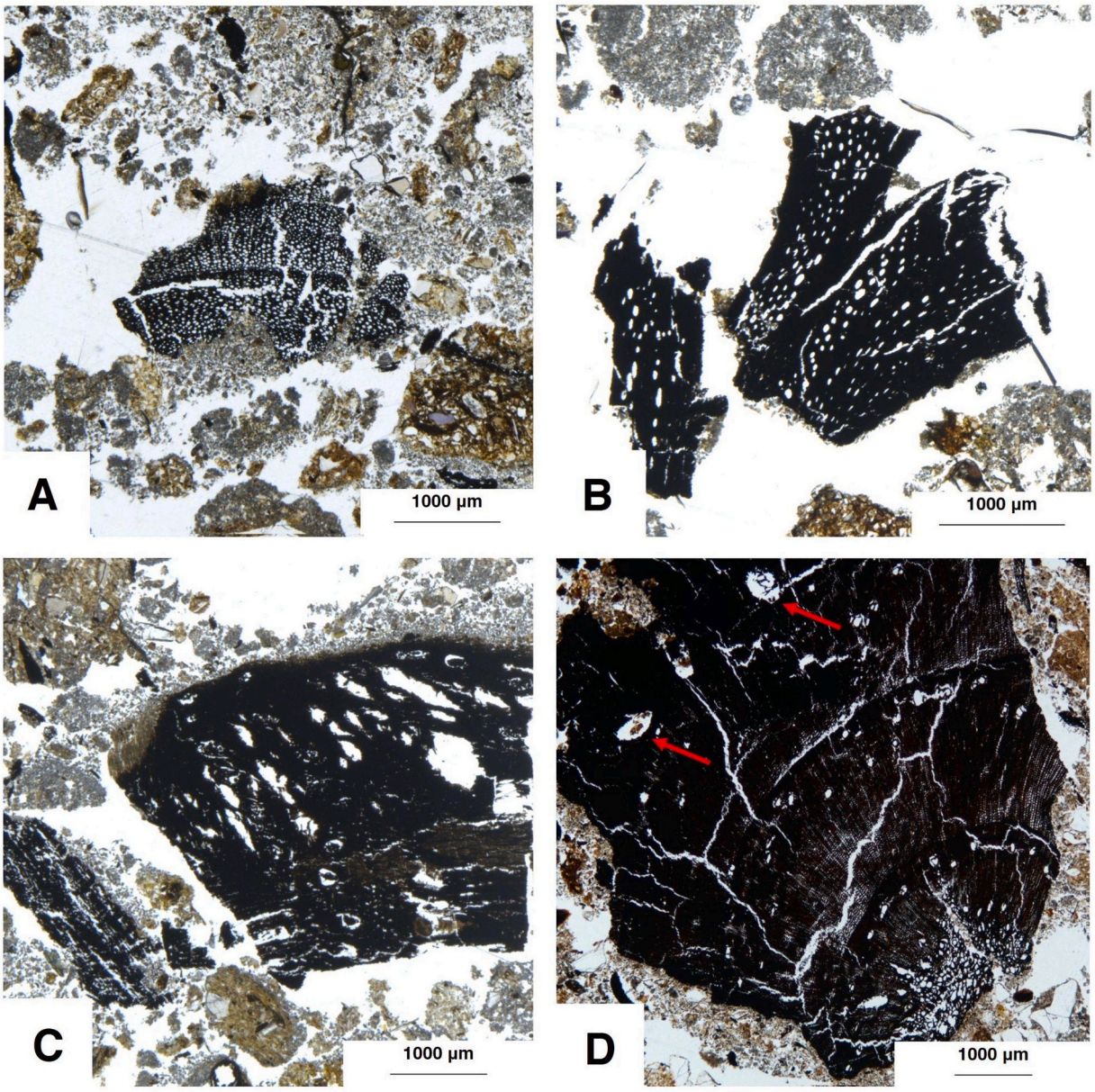

Fig. 8. Microphotographs (PPL) displaying representative charcoal fragments identified on thin sections. Cross sections of **A)** dicot, **B)** evergreen *Quercus*, **C)** deciduous *Quercus*, and **D)** *Pinus* sp., displaying the medulla, four annual growth rings, and two xylophagous galleries (red arrows). (For interpretation of the references to color in this figure legend, the reader is referred to the web version of this article.)

4.2. The mudbrick infill

The combustion layer is overlain by a ~60 cm-thick deposit composed of three superimposed layers of horizontally arranged mudbricks, which differ in colour, size, and arrangement. Micromorphological analysis shows that all mudbricks (MFT 5a, MFT 5b) share a compact silty-clayey groundmass with a massive structure, granostriated b-fabric, and an abundance of fine-to-coarse sand-sized subangular to subrounded quartz and slate. The primary differences among them relate to the type and abundance of voids, including vughs and vesicles, which reflect variations in the amount of water used during their production (Friesem et al. 2017; Cammas 2018). Additionally, some mudbricks exhibit a higher abundance of moldic voids, indicating the inclusion of plant temper in their fabrication, while others show fewer, suggesting a reliance on geogenic materials, such as quartz sand, as the main tempering agent (Love 2012; Friesem et al. 2017; Cammas 2018; Lorenzon et al. 2023).

Their mineralogical and geochemical composition, dominated by quartz, clay minerals, and feldspar, is characteristic of sediments derived from granite and slate lithologies, such as those found in the Tormes Valley, where CSV is located. The compositional variability appears to be primarily influenced by granulometry: clay minerals and quartz are more abundant in finer sediments (mud), whereas feldspar and quartz are predominant in coarser, sandy to pebbly sediments, including the lithoclasts present in mudbricks. This is also well represented by the PCA analysis (Fig. 10**C** and Fig. 10**D**), as in PC_1 SiO_2 (quartz) and Fe_2O_3, Al_2O_3 (major components of clay minerals) are inversely correlated. PC_2 seems to reflect changes in biophilic elements, CaO, LOI-Corg, P_2O_5 and SO_3, likely related to the use of plant temper for mudbrick manufacturing. PC_4 is interpreted as a marker for the presence of feldspar, as K_2O and Na_2O are the most abundant cations in feldspar composition.

Therefore, no substantial differences were found among the mudbricks, and their micromorphological, geochemical, and mineralogical

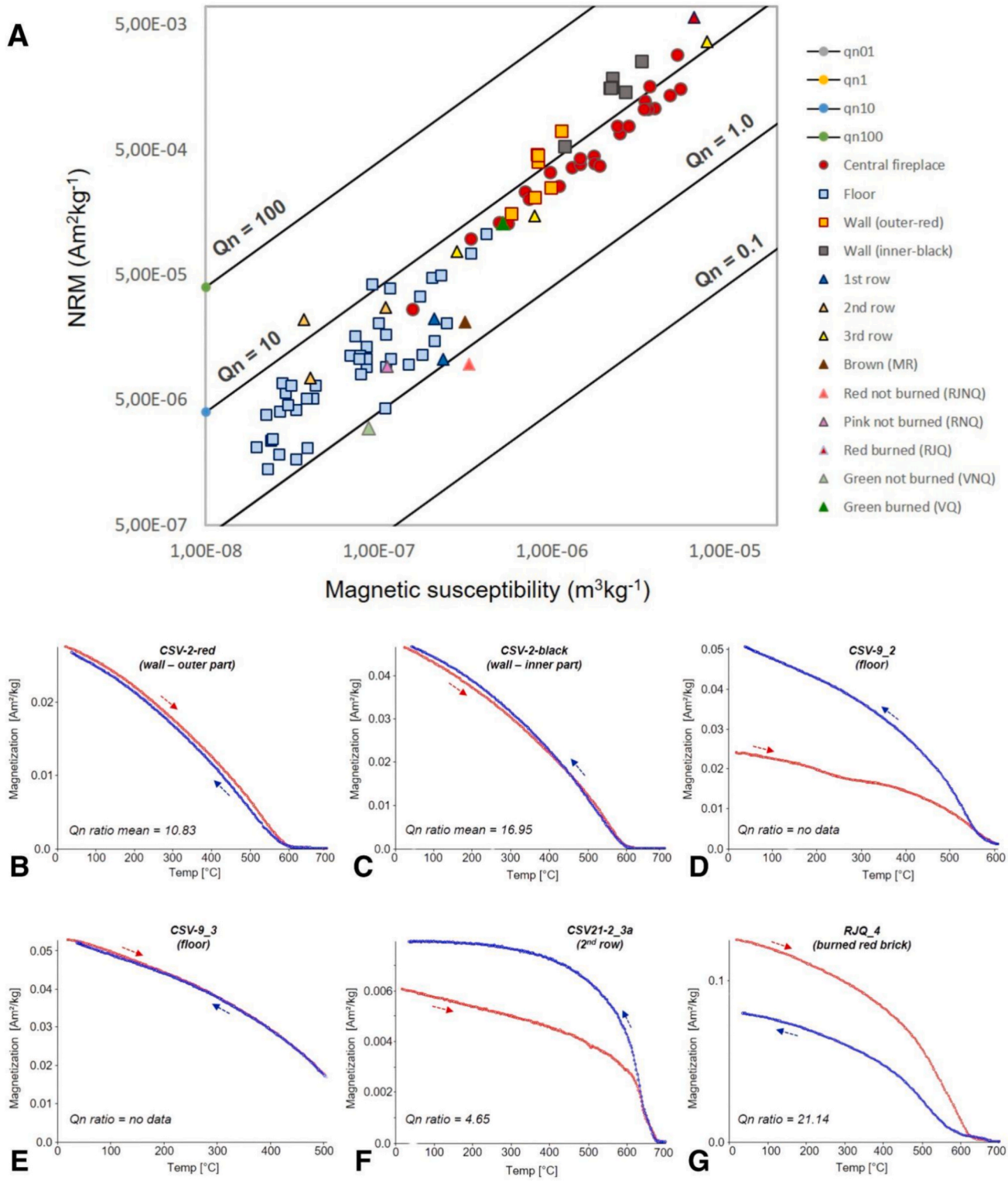

Fig. 9. A) The natural remanent magnetization (NRM) *vs* the magnetic susceptibility showing lines of constant Koenigsberger ratio (Q_n) between 0.1 and 100. The materials studied are plotted with different icons according to the legend. **B–G)** Representative thermomagnetic curves (magnetization *vs* temperature) for the studied materials. Heating (cooling) cycles are plotted in red (blue) with their respective arrows. The sample code, type of material and area of the house, Koenigsberger (Q_n) ratio values and intensity of magnetization are indicated for each sample. Detailed information is presented in the main text (Section 3.2.) and supplementary material S5. (For interpretation of the references to color in this figure legend, the reader is referred to the web version of this article.)

composition is consistent with previously analysed mudbricks from CSV (Tomé et al. 2024a). However, micromorphological data suggest that some of the mudbricks from the House 1 infill (MFU 2, MFU 7, MFU 5) may be unburnt or slightly affected by fire, while others (MFU 4, MFU 5) appear to have been significantly impacted by heat, as they display a bright red, rubified silty-clayey matrix (Forget et al. 2015). This aligns with field observations, through which mudbrick of different color ranges were registered.

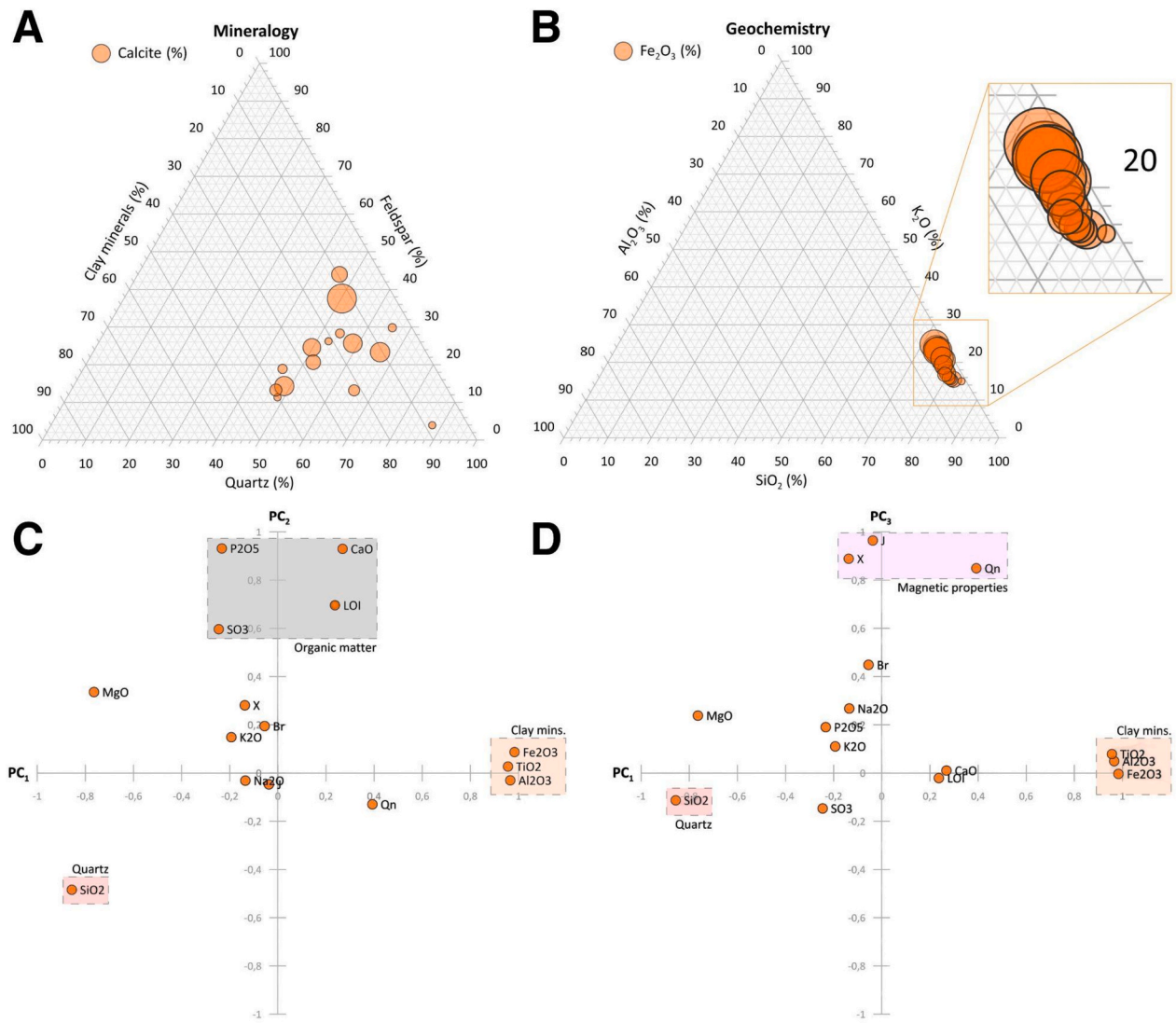

Fig. 10. Mineralogical (XRD) **(A)** and geochemical (XRF) **(B)** data of mudbrick samples from House 1 (note that the percentages are normalized to 100 %). Principal component analysis results represented by PC_1 *vs* PC_2 bivariate plot **(C)** and PC_1 *vs* PC_3 bivariate plot **(D)**. PC_1 explains the 30.7% of the geochemical variance of the analysed samples, PC_2 the 20.6% and PC_3 the 19.1%.

Notably, PC_3 (Fig. 10**D**) encompasses all the magnetic properties included in the PCA (Q_n, χ & J), indicating that the magnetic characteristics of the different mudbrick samples vary independently of their mineralogical and geochemical composition. This suggests that another factor, beyond elemental composition, is influencing the magnetic properties of the samples—specifically, the degree of thermal alteration or burning. In fact, magnetic properties data suggest that most of the analyzed samples were heated to some extent, but they show significant magnetic variability. Some, like the control mudbrick samples (supplementary material S1), exhibit high magnetic susceptibility, with reversibility up to 700 °C and high Q_n ratios (>10), indicating substantial heating (minimum of 700 °C), while others show no evidence of heating. The majority, however, carry a stable thermoremanent magnetization (TRM), suggesting they likely exceeded 600 °C (Fig. 9). These temperatures, ranging from 500 °C to 700 °C, have been previously documented in mudbricks affected by conflagration and destruction events in other archaeological contexts (Namdar et al. 2011; Forget et al. 2015).

These data suggest that most of the mudbricks from the House 1 infill were exposed to heat. But were they directly affected by the burning event in House 1, and if so, how? Micromorphological evidence provides key insights. Interspersed among the mudbricks are ~1 cm-thick layers of microscopic, fragmented, and disintegrated earth-based construction materials (e.g., mudbrick, clay floor), observed as both anorthic and disorthic silty-clayey nodules (MFT 2a, MFT 2b, MFT 5) with a random arrangement. These fragments are mixed with combustion-related features, including reworked aggregates of wood ash and abundant sand-sized, subrounded charcoal particles. Notably, no significant post-depositional processes—aside from insect bioturbation on charcoal fragments and recent root bioturbation—have been identified. In addition, the absence of rubified surfaces or substrates (black/red layers) rules out the occurrence of *in situ* fires between mudbricks (Mallol et al. 2013b, a; Aldeias et al. 2016). All these features indicate reworking and redeposition of charred combustion materials (Mentzer 2014; Mallol et al. 2017). As with the combustion deposit from the firing event, the lack of bioturbation in these inter-mudbrick layers suggests that subsequent layers of mudbricks were added quickly, minimizing any possible post-depositional disturbances. It is plausible that these combustion remains (MFT 12a) were adhered to mudbrick fragments (MFT 5a, 5b) and construction earth-based mortar (MFT 13) previously exposed to fire (Fig. 12**D**). This interpretation aligns with observations made during the excavation of House 1's mudbrick infill, as well as with the discrepancies in heating temperatures recorded by magnetic properties data.

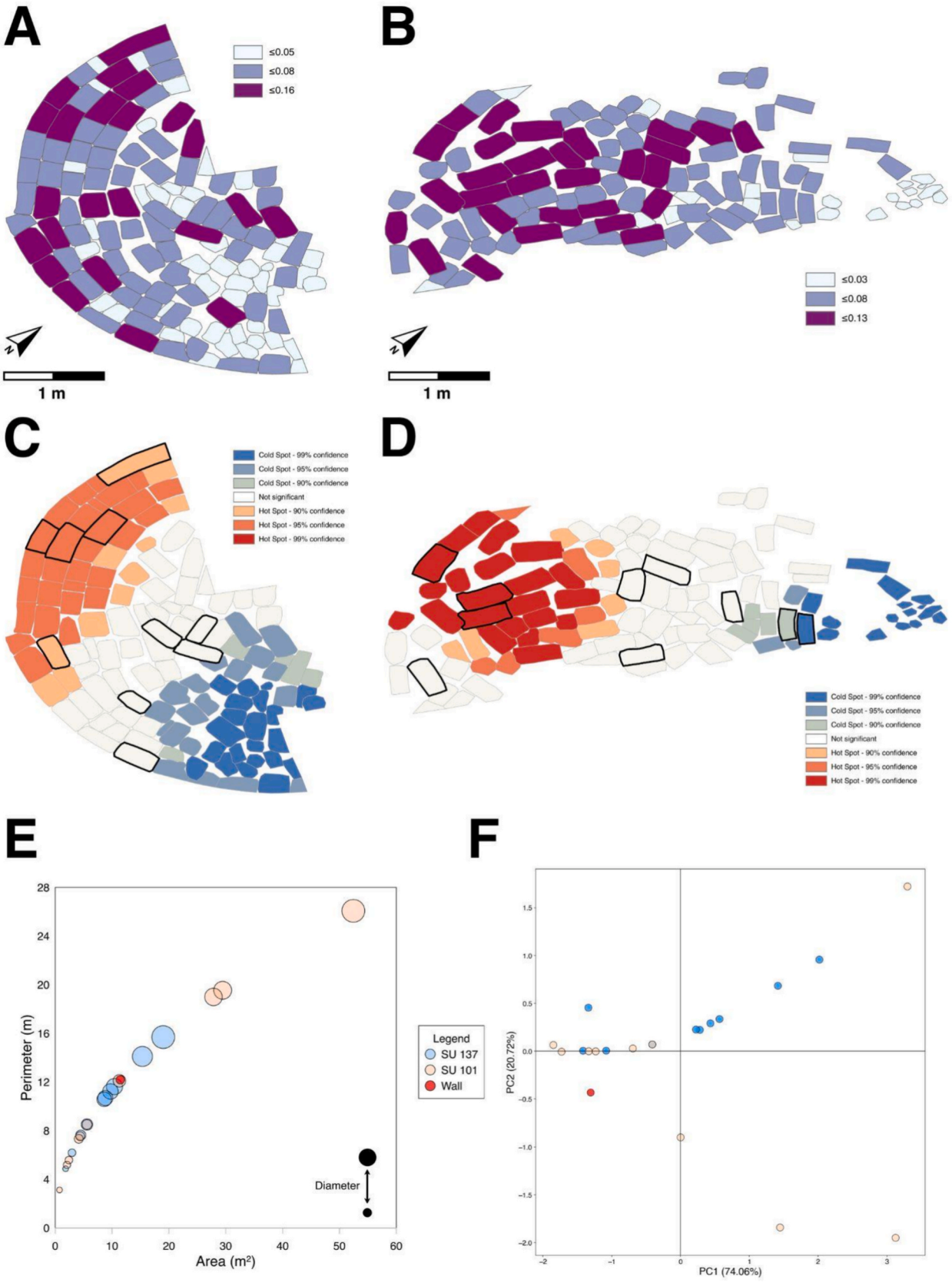

Fig. 11. Spatial and statistical data of the mudbrick infilling of House 1. **A)** Jenks classification results from SU 137. **B)** Jenks classification results from SU 101. **C)** Optimized Hotspot results from SU 137. Sampled mudbricks are represented with black edges. **D)** Optimized Hotspot results from SU 101. Sampled adobes are represented with black edges. **E)** Scatter plot representing morphological features of osculatrix perimeters by SU and wall. **F)** PCA applied to morphological features of osculatrix circumferences.

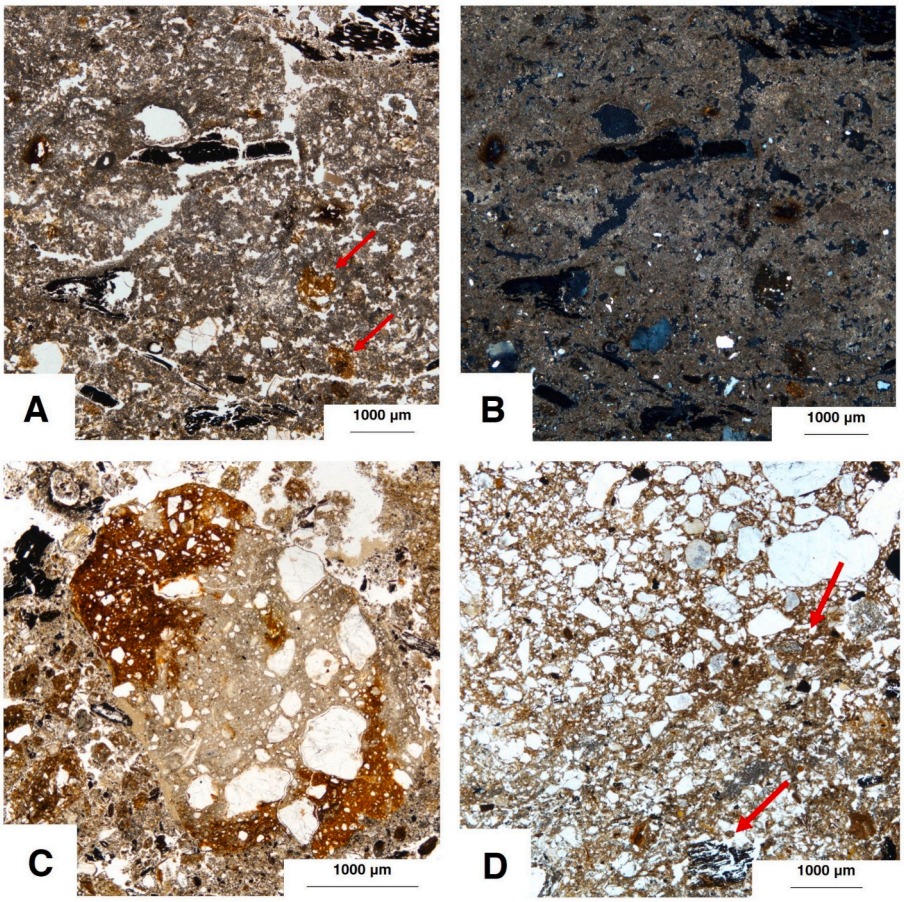

Fig. 12. Microphotographs highlighting key micromorphological features from the sequence of House 1. **A)** PPL. Massive, compact calcitic wood ash deposit containing a few fragments of earth-based construction material (red arrows) and subangular to subrounded charcoal fragments. The main porosity types are vughs and planes. **B)** XPL. Same field as **A**. Calcitic-crystallitic micromass with few sand-sized, subrounded quartz grains. **C)** PPL. Anorthic nodule of earth-based construction material, specifically a floor preparation fragment (MFT 1b), characterized by a light-yellow clayey matrix with abundant sand-sized, subrounded quartz grains. Note the reddened edges, indicative of uneven burning. It is embedded in a calcitic matrix with abundant charcoal fragments of varying sizes. **D)** PPL. Deposit located between mudbrick rows. Compact silty-sandy micromass containing ash aggregates and charcoal fragments (lower red arrow). Note the earth-based construction material (MFT 13) placed on top, compressing and deforming the underlying deposit (upper red arrow). (For interpretation of the references to color in this figure legend, the reader is referred to the web version of this article.)

How were the mudbricks heated? Data obtained through GIS-based morphological and spatial analyses of the infill mudbricks provide valuable insights. Specifically, measurements of the osculatrix circumferences of the mudbricks reveal key patterns (Fig. 11**E** and Fig. 11**F**). Among the analyzed mudbricks, a subset directly correlates with the osculatrix circumference of House 1's walls. This suggests that these mudbricks were likely part of House 1's original walls and were directly exposed to the burning event. Conversely, other mudbricks do not match the osculatrix circumference of House 1. Some of these have smaller circumferences, suggesting they may have been collected from ancillary structures, other building parts (e.g., floors, baseboards), smaller buildings, or even from different areas within CSV. Others have larger circumferences with minimal curvature, indicating they may have been recycled from rectangular buildings (i.e., Building 3), larger roundhouses, or other unknown structures within the settlement. Future GIS-based analyses of other buildings at CSV will help refine these hypotheses.

This evidence suggests that part of the mudbrick infill in House 1 originated from its own walls and was directly affected by heat *in situ*. Another portion was likely gathered from different areas across the village. This pattern is consistent with observations in both SUs 137 and 101. Further insights are provided by the Hotspot analysis of the mudbricks, which identifies two distinct clusters based on their area (Fig. 11**C** and Fig. 11**D**). Mudbricks located farther from the house's entrance are generally larger, while those closer to the entrance tend to be smaller. This distribution suggests that the infilling process began at the back of the house and progressed toward the entrance. Larger, more regular mudbricks may have been prioritized at the beginning of the process—which may have involved multiple people—, indicating greater care in their placement. This is also evident in both SUs 137 and 101.

Overall, our multi-proxy approach indicates that the mudbrick infilling of House 1 was likely a short-term depositional event. The process involved selecting mudbricks from two sources: those affected by the burning event (originally part of House 1's walls) and others collected from various locations within the settlement. This deliberate action sealed the combustion layer beneath the infill. The possible motivations for this practice are discussed in the following section.

4.3. *The context of House 1: Insights into settlement dynamics*

Our geoarchaeological study of House 1 reveals two key formation processes: 1) the burning event, which affected its roof, walls, and clay floor, and 2) the subsequent rapid infill of the structure using mudbricks from its own walls and other areas and/or buildings within CSV. The evidence indicates that these processes—the destruction by fire and the deliberate infilling with mudbricks—were interconnected, suggesting that they happened in a short period of time and, therefore, were likely

performed by members of an extended household.

Considering these findings, the intentionality behind these processes warrants further exploration. As discussed in Section 4.2, our data suggest that the infilling of House 1 was deliberate, leading to a rise in the floor level by approximately 60 cm. Interestingly, a hall for the house was then constructed, exactly at the height of the uppermost mudbrick layer in the infill. Our micromorphological data indicates that the ~1 cm-thick deposits between mudbricks likely do not correspond to use/occupation surfaces but rather to reworked charred combustion residues attached to earth-based construction material fragments. Furthermore, the absence of intense bioturbation indicates that the mudbrick layers were sealed quickly, one on top of the other. This rapid sealing is in contrast to what is observed in other buildings or areas at CSV, such as the abandonment deposits of House 2 and the Ancillary Structure (Tomé et al. 2024a), where intense bioturbation altered the original deposits. At CSV, bioturbation has been detected in areas that were unroofed or exposed, but no such activity was observed in the sequence of House 1.

Blanco-González et al. (2022) previously suggested that if the infill was indeed intentional, it may have been done to raise the house and construct again on top of the last mudbrick layer. In fact, a similar arrangement of mudbrick within roundhouses has previously been documented at other sites in the Duero Basin (Palol and Wattenberg 1974; Delibes de Castro et al. 1995). A closer examination of field stratigraphy at CSV can provide further clarity. Notably, the hall of House 1 was also elevated. Stratigraphic data reveal that the new hall entrance was built on top of a midden deposit located just outside House 1. This midden is stratigraphically correlated with Midden 1, which has been studied micromorphologically (Tomé et al. 2024b). Geoarchaeological data indicated that the midden was primarily formed through the repeated deposition of wood ash and charcoal, likely as the result of multiple hearth rake-out events.

The recurrent accumulation of ashes and discarded items, such as pottery fragments and faunal remains, led to the gradual uplift of the transit areas between the earthen buildings in the village. This is especially important considering that the volume of ash observed in the current stratigraphy does not reflect its original dimension, as these ash deposits may have undergone up to 90 % post-depositional compaction (Karkanas 2021). Therefore, it is reasonable to hypothesize that, as the level of the transit areas rose, House 1 and other earthen dwellings would have started to be partially covered by these midden deposits, potentially making the entrances to the buildings harder to access. As a result, the raising of House 1's level by reusing mudbricks from its walls and other buildings in CSV may have been the villagers' response to this challenge.

A closer examination of the stratigraphy of House 1 and other earthen dwellings at CSV may yield more valuable insights. Notably, on top of the third mudbrick infill layer of House 1, a ~8 cm-thick compact silty-clayey deposit was exhumed during the 2006 field season, covering the entire surface of the infill. While microstratification is not visible macroscopically, its thickness, granulometry, and color resemble other documented clay floors at CSV, including those in House 1 (from the floor sequence in the test pit) and in House 2 (Tomé et al. 2024a). Although further micromorphological analysis is needed to confirm this, it is plausible that this deposit represents a clay floor built on top of the mudbrick infill. If this is the case, the deliberate placement of mudbricks inside House 1 for the purpose of uplifting the building would be further supported. This could also explain the elevation of the entrance hall. However, the functions of House 1 likely changed over time, as evidenced by the absence of the central clay hearth in this upper layer (Blanco-González et al. 2017, Blanco-González et al., 2022).

Interestingly, a similar stratigraphic sequence can be suggested for House 2. Although it has not been fully excavated, a previous geoarchaeological study recorded the presence of a microstratified floor sequence above a mudbrick pavement (Tomé et al. 2024a). This mudbrick layer could have served a similar purpose to that of House 1's mudbrick infill: uplifting the house. Remarkably, a similar mudbrick infill was also documented in Building 3, with an underlying midden deposit (Blanco-González et al. 2023a). In addition, the lowest layer in the test pit excavated in House 1 also revealed a mudbrick pavement. While further fieldwork and geoarchaeological analysis are needed to test this hypothesis, it is clear that the presence of mudbricks inside houses, either overlain or underlain by clay floors, seems to be a common formation pattern across CSV. This, combined with the presence of thick, multi-stratified midden deposits interspersed among the dwellings, supports the interpretation that the dwellings could have been intentionally uplifted as the level of the surrounding transit areas also rose.

4.4. The cultural significance of house burning

The burning of House 1 has previously been interpreted by Blanco-González et al. (2022) as intentional. This account was based on field data, which showed that most items inside the house were removed prior to or immediately after the conflagration event, and that the house was carefully emptied before the mudbrick infill was placed. This is further supported by the absence of the conflagration layer outside the walls of House 1. The data presented here also point towards this interpretation, indicating that the intentional sealing of the house likely occurred in rapid succession following the conflagration event.

If House 1 was intentionally burnt, what could have been the rationale behind this practice? Experimental studies have demonstrated that arsoning an earth-based dwelling is a challenging task, requiring a prolonged fire and large amounts of fuel (Bankoff and Winter 1979; Shaffer 1993; Forget et al. 2015; Forget and Shahack-Gross 2016; Gheorghiu 2017; Johnston et al 2018, 2019; Kreimerman and Shahack-Gross 2019). Therefore, specific socioeconomic and cultural factors must have driven the intentional burning of House 1. Shaffer (1993) proposed that house burning practices at the Neolithic site of Piana di Curinga could serve to harden and improve the properties of wattle-and-daub as construction material, which was sun-dried and more susceptible to degradation, before being reused in new constructions. In fact, evidence from other archaeological contexts suggests that ashes were used as construction mortars (Matthews 2010; Pastor Quiles 2021), likely due to their hydrophobic properties, which help repel water and moisture (Matthews 2010). This technological interpretation of fire as a transformative agent (Matthews 2016) for enhancing construction materials aligns with theoretical models that explore the social, cultural, and economic implications of technological practices as driving forces behind human behavior (Dobres 2000; Sillar and Tite 2000; Schiffer 2003; Schiffer et al. 2001; Skibo and Schiffer 2008).

In the specific case of CSV, this interpretative background appears particularly pertinent, as we have evidence suggesting that after the walls were burnt, they were dismantled and used to fill the house, likely to build a new clay floor and foundation for the next construction phase. As discussed above, the lack of phytoliths in the ashy layer (SU 140) might also indicate the removal and recycling of the thatched roof. Additionally, beyond House 1, the systematic occurrence of burnt dwellings documented at CSV from its foundational phases (Blanco-González et al. 2017) suggests that this may have been a more widespread practice within the settlement. Other coeval villages of the Duero Basin exhibit similar dynamics. At the Western part of this region, Ledesma (Salamanca), showed a complete burnt roundhouse (Benet et al 1991). At Soto de Medinilla (Valladolid), evidence of deliberate burning is present from the earliest occupation level, affecting individual houses (Palol and Wattenberg 1974). At La Mota (Medina del Campo), a substantial assemblage of vessels and fragments of unguentaria—among other objects—was recovered directly above a burnt floor (Seco and Treceño 1993). Similar evidence has also been documented at Cuéllar (Segovia) (Barrio 1993).

While we cannot assert this with certainty, the model proposed by Shaffer (1993) may be consistent with the archaeological context at CSV, where our data support the reuse of burnt earth-based construction

materials in new architectural phases. The potential recurrence of this construction strategy—based on the circular reuse of materials over time to minimize waste or optimize resources (Romankiewicz 2023)—appears not only at House 1 but also in other dwellings from CSV (Blanco-González et al., 2017) and from other contemporary sites. At Soto de Medinilla, for instance, Houses 2 and 7 in the final phase of the Early Iron Age show overlapping mudbrick floors (Palol and Wattenberg 1974), while at La Mota (Medina del Campo), similar practices were documented in the construction of a square-shaped building (Blanco-García and Retuerce 2010). These patterns suggest the existence of a consistent architectural tradition that persisted over time and extended beyond a single settlement. Future excavations at CSV and other Early Iron Age sites along the Duero Basin will be key to testing this hypothesis.

The arsoning and subsequent rebuilding of House 1—and potentially of other dwellings at CSV and across the Duero Basin—may also be understood as part of broader household maintenance practices. In fact, ethnoarchaeological studies have shown that the decision to fully renovate or rebuild a dwelling can be part of regular maintenance practices when a house is no longer considered to be in optimal condition as to be refurbishable. This may involve dismantling the existing structure and reusing architectural components in the construction of a new building on the same spot (Brooks 1993). These practices reflect a dynamic approach to architectural continuity, where renewal is not necessarily a sign of abandonment but of spatial conception and prolonged occupation. Moreover, geo-ethnoarchaeological observations indicate that maintenance tasks within domestic spaces often go beyond practical repair and are embedded in broader social contexts. Floor replastering activities, for instance, may follow seasonal cycles or be performed in response to culturally significant events, such as communal festivities, religious rituals, or key milestones within the household life-cycle (Matthews 2005; Boivin 2000). In fact, recurrent maintenance activities (i.e., floor sweeping and repaving) have previously been documented at CSV (Tomé et al., 2024a). As such, it is plausible to propose that the burning of houses represented a major form of maintenance and renewal, which although potentially triggered by practical needs, was also likely associated with social practices related to the continuity and the community's understanding of the inhabited space.

In this light, the burning of dwellings likely carried significant cultural meanings for the households inhabiting and maintaining these spaces. Blanco-González et al. (2022) have suggested a symbolic dimension to the burning of House 1 at the end of its life cycle, evidenced by the meticulous cleaning of the dwelling afterward and the presence of only selected, valuable items left inside. This aligns with models proposed by various authors (Stevanović 1997; Chapman 1999; Gheorghiu 2008; Tringham 2013; Russell et al. 2014; Sánchez Polo 2021), who interpret house burning as a form of closure—marking the end of a building's functional life cycle and/or the life cycle of its inhabitants. Ethnographic examples also show similar practices, where the death of a prominent individual in a community was followed by the burning of their house (Springer 2009; Moore 2012). Furthermore, Chapman (1999: 122) suggested that the deliberate burning of houses, along with the reuse of their materials in new constructions built atop ancestral dwellings, may have served as a powerful material expression of continuity and exchange between the living and their ancestors within households. In a similar vein, Tringham (2013: 99) proposed that the "euthanizing" of a house—through closure rituals, feasting, dismantling, and infilling—might be understood as a socially meaningful act, one that potentially brought people together, nurtured shared memories, and contributed to the perceived continuity of place.

However, to achieve more accurate interpretations of house burning practices at CSV, future research must focus on extending excavations across the site and thoroughly analyzing other dwellings and neighbourhoods. This would allow us to determine whether the hypotheses proposed in this paper—such as the intentional dismantling and reuse of mudbricks to elevate house levels—are consistent across the settlement. Moreover, integrating geoarchaeological and spatial data from multiple buildings would provide a more comprehensive understanding of on-site dynamics and cultural practices at CSV. Crucially, situating this case study within the wider phenomenon of house burning across the prehistoric world requires comparative, high-resolution geoarchaeological research across diverse cultural and environmental settings. Identifying recurring formation processes and distinguishing them from context-specific practices will be essential for disentangling the socioeconomic, functional, and cultural dimensions of house burning across regions and time periods.

5. Conclusions

In this paper, we have analyzed the sequence of House 1 at CSV using a multi-proxy geoarchaeological approach, including archaeological soil micromorphology (with charcoal analysis on thin sections), magnetic properties analyses, XRD and XRF, and GIS-based morphological and spatial analyses of mudbricks. Our primary goal was to investigate the formation processes associated with the burning of House 1 and its subsequent sealing. The results indicate that the conflagration of House 1 was likely a high-intensity event, prompting the collapse of the roof and the intense burning of its walls and floor. This produced a thick, intact wood ash layer rich in combustion debris. Shortly afterward, our data suggest that House 1 was deliberately infilled with recycled mudbricks from its dismantled walls and, potentially, other dwellings across the settlement. This practice likely served functional aims—such as elevating the floor level and preparing the dwelling for rebuilding—while also contributing to broader processes of domestic renewal and maintenance.

While these findings deepen our understanding of architectural and settlement dynamics at CSV, they also contribute to broader archaeological issues about the roles of social maintenance and circular socioeconomic practices in prehistoric household life. The potential interplay between practical and cultural motivations—such as the reuse of building materials, lifecycle closure, and social continuity—suggests that house burning may have worked as a meaningful cultural practice within long-term domestic and communal rhythms. The evidence from House 1 points to a purposeful renewal of the domestic space, indicating that house burning may have served as a socially embedded practice of maintenance and renewal within household and community life.

Furthermore, the case of CSV contributes to a growing body of research that approaches burnt domestic contexts not merely as destruction events, but as active practices in the long-term shaping of the domestic social space. Expanding the investigation to other dwellings at CSV and conducting comparative geoarchaeological studies across diverse cultural and environmental settings will be essential to identify recurring patterns and local variations. Such integrative approaches will help clarify the utilitarian, symbolic, cultural, and social roles that house burning played in prehistoric domestic life.

Declaration of Generative AI and AI-assisted technologies in the writing process

During the preparation of this work the authors used Chat GPT in order to improve English grammar of some parts of the text. After using this tool/service, the authors reviewed and edited the content as needed and take full responsibility for the content of the publication.

CRediT authorship contribution statement

Laura Tomé: Writing – original draft, Visualization, Investigation, Formal analysis, Conceptualization. **Antonio Blanco-González:** Writing – review & editing, Visualization, Supervision, Resources, Project administration, Funding acquisition, Conceptualization. **Eneko Iriarte:** Writing – review & editing, Writing – original draft,

Visualization, Validation, Resources, Investigation, Formal analysis, Conceptualization. **Ángel Carrancho:** Writing – review & editing, Writing – original draft, Visualization, Investigation, Formal analysis. **Natalia García-Redondo:** Writing – review & editing, Investigation, Formal analysis, Conceptualization. **Santiago Sossa-Ríos:** Writing – review & editing, Writing – original draft, Visualization, Investigation, Formal analysis. **Alejandra Sánchez-Polo:** Writing – review & editing, Writing – original draft, Visualization, Investigation. **María Martín-Seijo:** Writing – review & editing, Writing – original draft, Visualization, Investigation, Formal analysis. **Carolina Mallol:** Writing – review & editing, Visualization, Validation, Supervision, Resources, Investigation, Formal analysis, Conceptualization.

Funding

This research paper is a component of LT's PhD thesis, and all authors agree. This research was funded by the Spanish Ministry of Science and Innovation (Project PID2019-104349GA-I00, AEI/https://doi.org/10.13039/501100011033) and a predoctoral contract awarded to LT (TESIS2021010119), co-funded by the Agencia Canaria de Investigación, Innovación y Sociedad de la Información de la Consejería de Universidades, Ciencia e Innovación y Cultura, and by the European Social Fund Plus (ESF+) Integrated Operational Program of the Canary Islands 2021–2027, Axis 3 Priority Theme 74 (85 %). LT was also the beneficiary of a grant (EST2024010006) for a short stay abroad within an official PhD program in the Canary Islands, co-funded by the European Social Fund Plus, for the year 2024. AC acknowledges the project PID2019105796GB-I00 of the Agencia Estatal de Investigación (AEI/https://doi.org/10.13039/501100011033) and Junta de Castilla y León (project BU037P23) and the European Research and Development Fund (ERDF). SS-R is the beneficiary of a predoctoral research contracting grant awarded by the Generalitat Valenciana (ACIF/2021/407). ASP is the beneficiary of a postdoctoral Juan de la Cierva contract (FJC2021-046615-I), funded by MCIN/AEI/https://doi.org/10.13039/501100011033 and European Union NextGenerationEU/ PRTR. The MMS archaeobotanical research was supported by the grant CNS2023-144343 funded by MICIU/AEI /https://doi.org/10.13039/501100011033 and European Union NextGenerationEU/PRTR.

Declaration of competing interest

The authors declare that they have no known competing financial interests or personal relationships that could have appeared to influence the work reported in this paper.

Acknowledgements

The authors would like to thank Cristina Alario, Carlos Macarro and Juan Jesús Padilla for field supervision, as well as the Cerro de San Vicente excavation team for their field work. We thank Carlos Duarte Simões for supervising LT's international research stay at ICArEHB (International Center for Archaeology and the Evolution of Human Behaviour, Universidade do Algarve), where the micromorphological analysis for this article was conducted. We thank Alejandro Mayor and Javier Davara for reading the draft, and William Molina for his assistance with Python. We are thankful to the CENIEH and Wagner Petrographic personnel for thin section manufacture, to the I + D + i Scientific-Technological Center (Universidad de Burgos) personnel for performing mineralogical and geochemical analyses (XRD and XRF), and to the PREHUSAL Research Group for its role in facilitating the production of thin sections in the Nucleus Laboratory (USAL).

Appendix A. Supplementary material

Supplementary data to this article can be found online at https://doi.org/10.1016/j.jaa.2025.101711.

References

Aldeias, V., Dibble, H.L., Sandgathe, D., et al., 2016. How heat alters underlying deposits and implications for archaeological fire features: a controlled experiment. J. Archaeol. Sci. 67, 64–79. https://doi.org/10.1016/j.jas.2016.01.016.

Amadio, M., Bombardieri, L., 2019. Abandonment processes at Middle Bronze Age Erimi: a multi-scalar approach. Antiquity 93, e9. https://doi.org/10.15184/aqy.2019.29.

Akkemik, Ü., Yaman, B., 2012. Wood Anatomy of Eastern Mediterranean Species. Kessel Publishing House, Remagen.

Bailey, G., 2007. Time perspectives, palimpsests and the archaeology of time. J. Anthropol. Archaeol. 26, 198–223. https://doi.org/10.1016/j.jaa.2006.08.002.

Balbo, A.L., Iriarte, E., Arranz, A., Zapata, L., Lancelotti, C., et al., 2012. Squaring the circle. social and environmental implications of pre-pottery neolithic building technology at Tell Qarassa (South Syria). PLoS One 7 (7), e42109. https://doi.org/10.1371/journal.pone.0042109.

Bankoff, H.A., Winter, F.A., 1979. A House-burning in Serbia: what do burned remains tell an archaeologist? Archaeology 32, 8–14.

Barrio, J., 1993. Estratigrafía y desarrollo poblacional en el yacimiento prerromano de la plaza del Castillo (Cuéllar, Segovia). In: Arqueología Vaccea. Estudios sobre el mundo prerromano en la cuenca media del Duero. Junta de Castilla y León, Valladolid, pp. 173–212.

Benet N, Jiménez MC, Rodríguez, B (1991) Arqueología en Ledesma, una primera aproximación: la excavación en la Plaza de San Martín. In Del Paleolítico a la Historia, Museo de Salamanca. Salamanca, pp. 117-136.

Binford, L.R., 1981. Behavioral Archaeology and the "Pompeii Premise.". J. Anthropol. Res. 37, 195–208. https://doi.org/10.1086/jar.37.3.3629723.

Blanco-García, J.F., Retuerce, M., 2010. Últimas intervenciones arqueológicas en el cerro de La Mota (Medina del Campo, Valladolid). Vaccea Anuario 3, 77–79.

Blanco-González, A., Alario García, C., Macarro Alcalde, C., 2017. The Earliest villages in Iron Age Iberia (800-400 BC): a view from Cerro de San Vicente (Salamanca, Spain). Documenta Praehistorica 44, 386.

Blanco-González, A., Padilla Fernández, J.J., Alario García, C., et al., 2022. Un singular ambiente doméstico del Hierro I en el interior de la península ibérica: la casa 1 del Cerro de San Vicente (Salamanca, España). Trabprehist 79, 346–361. https://doi.org/10.3989/tp.2022.12303.

Blanco-González, A., Padilla Fernández, J.J., Alario García, C., et al., 2024. Arqueología doméstica del Hierro I meseteño: excavaciones de 2018 en el Cerro de San Vicente (Salamanca, España). Complutum 35, 103–125. https://doi.org/10.5209/cmpl.95926.

Blanco-González, A., Padilla Fernández, J.J., Alario García, C., et al., 2023a. Un santuario doméstico del siglo VII a. C. de culto a Hathor-Astarté en el Cerro de San Vicente (Salamanca, España). Trabprehist 80, e06–e. https://doi.org/10.3989/tp.2023.12321.

Blanco-González, A., Padilla-Fernández, J.J., Dorado-Alejos, A., 2023b. Mobile craftspeople and orientalising transculturation in seventh-century BC Iberia. Antiquity 1–19. https://doi.org/10.15184/aqy.2023.96.

Bloemendal, J., King, J.W., Hall, F.R., Doh, S.J., 1992. Rock magnetism of late Neogene and Pleistocene deep-sea sediments: Relationship to sediment source, diagenetic processes and sediment lithology. J. Geophys. Res. 97 (B4), 4361–4375.

Boivin, N., 2000. Life rhythms and floor sequences: excavating time in rural Rajasthan and Neolithic Çatalhöyük. World Archaeol. 31, 367–388. https://doi.org/10.1080/00438240009696927.

Brooks, R.L., 1993. Household abandonment among sedentary Plains societies: behavioral sequences and consequences in the interpretation of the archaeological record. In: Cameron, C.M., Tomka, S.A. (Eds.), The Abandonment of Settlements and Regions: Ethnoarchaeological and Archaeological Approaches. Cambridge University Press, Cambridge, pp. 178–187. https://doi.org/10.1017/cbo9780511735240.

Cabanes, D., 2020. Phytolith analysis in paleoecology and archaeology. In: Handbook for the Analysis of Micro-Particles in Archaeological Samples. Springer International Publishing, Cham, pp. 255–288. https://doi.org/10.1007/978-3-030-42622-4_11.

Cammas, C., 2018. Micromorphology of earth building materials: toward the reconstruction of former technological processes (Protohistoric and Historic periods). Quat. Int. 483, 160–179. https://doi.org/10.1016/j.quaint.2018.01.031.

Celestino Pérez, S., Fernández Freire, C., Walid Sbeinati, S., 2003. La funcionalidad de Cancho Roano. In: Celestino Pérez, S. (Ed.), Cancho Roano IX. Los materiales arqueológicos II. Junta de Extremadura, Mérida, pp. 299–358.

Cessford C, Near J (2005) Fire, Burning and Pyrotechnology at Çatalhöyük. In: Hodder I (ed) Çatalhöyük Perspectives: Themes from the 1995-9 Seasons. Çatalhöyük Research Project, McDonald Institute Monographs/British Institute of Archaeology at Ankara, Cambridge/London, pp 171–182.

Chapman, J., 1999. Deliberate house-burning in the prehistory of Central and Eastern Europe. Glyfer Och Arkeologiska Rum: En Vänbok till Jarl Nordbladh 44, 113–126.

Chapon, L., Padilla-Fernández, J.J., Dorado-Alejos, A., Blanco-González, A., 2024. Iron Age connectivity revealed by an assemblage of Egyptian Faience in Central Iberia. Eur. J. Archaeol. 1–23. https://doi.org/10.1017/eaa.2024.1.

Courty, M.-A., 2001. Microfacies Analysis Assisting Archaeological Stratigraphy. In: Goldberg, P., Holliday, V.T., Reid Ferring, C. (Eds.), Earth Sciences and Archaeology. Springer US, pp. 205–239.

Cutillas-Victoria, B., Lorenzon, M., Rodríguez González, E., Celestino Pérez, S., 2024. Hierarchical organization and skilled workforces for constructing the Tartessic earthen building at Casas del Turuñuelo (Guareña, Spain). Sci. Rep. 14, 1–15. https://doi.org/10.1038/s41598-024-70374-x.

Delibes de Castro G, Romero Carnicero F, Ramírez Ramírez ML (1995) El poblado 'céltico' de El Soto de Medinilla (Valladolid). In: Delibes de Castro G, Escudero Navarro Z, Arturo RCFM (eds) Arqueología y medio ambiente. El primer milenio a.C.

en el Duero Medio. Junta de Castilla y León, Consejería de Cultura y Turismo, Valladolid, pp 149–177.
Diwan, G., 2020. GIS-Based comparative archaeological predictive models: a first application to Iron Age sites in the Bekaa (Lebanon). Mediter. Archaeol. Archaeom. 20 (2), 143–158.
Dobres, M.A., 2000. Technology and Social Agency: Outlining a Practice Framework for Archaeology. Blackwell, Oxford.
Driessen, J. (Ed.), 2013a. Destruction: Archaeological, Philological and Historical Perspectives. Presses universitaires de Louvain, Louvain-la-Neuve.
Driessen, J., 2013b. Time Capsules? Destructions as Archaeological Phenomena. In: Driessen, J. (Ed.), Destruction: Archaeological, Philological and Historical Perspectives. Presses universitaires de Louvain, Louvain-la-Neuve, pp. 9–26.
Forget, M.C.L., Regev, L., Friesem, D.E., Shahack-Gross, R., 2015. Physical and mineralogical properties of experimentally heated chaff-tempered mud bricks: Implications for reconstruction of environmental factors influencing the appearance of mud bricks in archaeological conflagration events. J. Archaeol. Sci. Rep. 2, 80–93. https://doi.org/10.1016/j.jasrep.2015.01.008.
Forget, M.C.L., Shahack-Gross, R., 2016. How long does it take to burn down an ancient Near Eastern city? The study of experimentally heated mud-bricks. Antiquity 90, 1213–1225. https://doi.org/10.15184/aqy.2016.136.
Friede, H.M., Steel, R.H., 1980. Experimental burning of traditional Nguni huts. Afr. Stud. 39, 175–181. https://doi.org/10.1080/00020188008707557.
Friesem, D.E., 2018. Geo-ethnoarchaeology of fire: Geoarchaeological investigation of fire residues in contemporary context and its archaeological implications. Ethnoarchaeology 10, 159–173. https://doi.org/10.1080/19442890.2018.1510616.
Friesem, D.E., Karkanas, P., Tsartsidou, G., Shahack-Gross, R., 2014a. Sedimentary processes involved in mud brick degradation in temperate environments: a micromorphological approach in an ethnoarchaeological context in northern Greece. J. Archaeol. Sci. 41, 556–567. https://doi.org/10.1016/j.jas.2013.09.017.
Friesem, D.E., Tsartsidou, G., Karkanas, P., Shahack-Gross, R., 2014b. Where are the roofs? a geo-ethnoarchaeological study of mud brick structures and their collapse processes, focusing on the identification of roofs. Archaeol. Anthropol. Sci. 6, 73–92. https://doi.org/10.1007/s12520-013-0146-3.
Friesem, D.E., Wattez, J., Onfray, M., 2017. Earth Construction Materials. In: Nicosia, C., Stoops, G. (Eds.), Archaeological Soil and Sediment Micromorphology. John Wiley & Sons, Oxford, pp. 99–110.
García-Redondo, N., Calvo-Rathert, M., Carrancho, Á., et al., 2021. Further evidence of high intensity during the levantine iron age anomaly in Southwestern Europe: full vector archeomagnetic dating of an early iron age dwelling from Western Spain. J. Geophys. Res. [Solid Earth] 126. https://doi.org/10.1029/2021jb022614.
Gheorghiu, D., 2017. 3 Building and burning: the Construction and Combustion of Chalcolithic Dwellings in the lower Danube and the Eastern Carpathian areas from the Perspective of Experimental Archaeology. In: Western-Pontic Culture Ambience and Pattern. De Gruyter Open Poland, pp. 33–52.
Gheorghiu, D., 2019. Architectures of Fire: the pyro-proximities of the Chalcolithic Dwelling. In: Gheorghiu, D. (Ed.), Architectures of Fire. Archaeopress Archaeology, Oxford, England, pp. 30–47.
Gheorghiu, D., 2008. Looking for a methodology burning wattle and daub housing structures – a preliminary report on an archaeological experiment. Natl. Univ. Arts.
Goldberg, P., Miller, C.E., Schiegl, S., et al., 2009. Bedding, hearths, and site maintenance in the Middle Stone Age of Sibudu Cave, KwaZulu-Natal, South Africa. Archaeol. Anthropol. Sci. 1, 95–122. https://doi.org/10.1007/s12520-009-0008-1.
Gordon, D.H., 1953. Fire and the sword: the technique of destruction. Antiquity 27, 149–152. https://doi.org/10.1017/s0003598x00024790.
Harrison, K., 2013. The application of forensic fire investigation techniques in the archaeological record. J. Archaeol. Sci. 40, 955–959. https://doi.org/10.1016/j.jas.2012.08.030.
Harvig, L., Kveiborg, J., Lynnerup, N., 2015. Death in flames: Human remains from a domestic house fire from early iron age, Denmark. Int. J. Osteoarchaeol. 25, 701–710. https://doi.org/10.1002/oa.2335.
Jenks, G.F., 1967. The data model concept in statistical mapping. In: Frenzel, K. (Ed.), International Yearbook of Cartography VII. Liverpool, pp. 186–190.
Johnston S, et al. (2018) The Experimental Building, Burning and Excavation of a two-Storey Trypillia House, In Materiality and identity in Pre- and Protohistoric Europe. Homage to Cornelia-Magda Lazarovici. Suceava: The Bucovina Museum, Karl A. Romstorfer Publishing House: pp. 397–434.
Johnston, S., et al., 2019. The Nebelivka experimental house construction and house-burning, 2014–2015. Bulgarian e-J. Arch. 9, 61–90.
Julivert M, Fontboté JM, Ribeiro A, Conde (1972). Mapa tectónico de la Península Ibérica y Baleares, escala 1:1.000.000. Instituto Geológico y Minero de España, Madrid.
Karkanas, P., 2021. All about wood ash: Long term fire experiments reveal unknown aspects of the formation and preservation of ash with critical implications on the emergence and use of fire in the past. J. Archaeol. Sci. 135, 105476. https://doi.org/10.1016/j.jas.2021.105476.
Kovács, G., Vicze, M., Pető, Á., 2023. Fires of a house—burning events in a Middle Bronze Age Vatya house as evidenced by soil micromorphological analysis of anthropogenic sediments. Land 12, 159. https://doi.org/10.3390/land12010159.
Kreimerman, I., Garfinkel, Y., Hasel, M.G., Shahack-Gross, R., 2022. High-resolution investigation of a conflagration event in the North-East Temple at Lachish via integration of forensic, stratigraphic and geoarchaeological evidence: a model for studying architectural destruction by fire. J. Archaeol. Sci. Rep. 46, 103705. https://doi.org/10.1016/j.jasrep.2022.103705.
Kreimerman, I., Shahack-Gross, R., 2019. Understanding conflagration of one-story mud-brick structures: an experimental approach. Archaeol. Anthropol. Sci. 11, 2911–2928. https://doi.org/10.1007/s12520-018-0714-7.
Kruger, R.P., 2015. A burning question or, some half-baked ideas: patterns of sintered daub creation and dispersal in a modern wattle and daub structure and their implications for archaeological interpretation. J. Archaeol. Method Theory 22, 883–912. https://doi.org/10.1007/s10816-014-9210-2.
Lee, J., Wong, D., 2001. Statistical analysis with ArcView GIS. John Wiley & Sons, New York.
Leonhardt, R., 2006. Analyzing rock magnetic measurements: the RockMagAnalyzer 1.0 software. Comput. Geosci. 32, 1420–1431. https://doi.org/10.1016/j.cageo.2006.01.006.
Lin, H., Chen, Z., 2023. Spatiotemporal G Statistical Analytics. In: Jay, L. (Ed.), Spatiotemporal Analytics. CRC Press, pp. 113–125.
Lorenzon, M., Cutillas-Victoria, B., Itkin, E., Fantalkin, A., 2023. Masters of mudbrick: Geoarchaeological analysis of Iron Age earthen public buildings at Ashdod-Yam (Israel). Geoarchaeology. https://doi.org/10.1002/gea.21977.
Love, S., 2012. The geoarchaeology of mudbricks in architecture: a methodological study from Çatalhöyük, Turkey: Geoarchaeology of mudbricks in architecture. Geoarchaeology 27, 140–156. https://doi.org/10.1002/gea.21401.
Lucas, G., 2004. The Archaeology of Time, first ed. Routledge, London, England.
Lucas, G., 2008. Time and archaeological event. Camb. Archaeol. J. 18, 59–65. https://doi.org/10.1017/s095977430800005x.
Macarro Alcalde C, Alario García C (2012) Los orígenes de Salamanca. El poblado protohistórico del Cerro de San Vicente. Centro de Estudios Salmantinos, Salamanca.
Mallol, C., Hernández, C.M., Cabanes, D., et al., 2013a. Human actions performed on simple combustion structures: an experimental approach to the study of Middle Palaeolithic fire. Quat. Int. 315, 3–15. https://doi.org/10.1016/j.quaint.2013.04.009.
Mallol, C., Hernández, C.M., Cabanes, D., et al., 2013b. The black layer of Middle Palaeolithic combustion structures. Interpretation and archaeostratigraphic implications. J. Archaeol. Sci. 40, 2515–2537. https://doi.org/10.1016/j.jas.2012.09.017.
Mallol, C., Mentzer, S.M., Miller, C.E., 2017. Combustion features. In: Nicosia, C., Stoops, G. (Eds.), Archaeological Soil and Sediment Micromorphology. Wiley Blackwell, Oxford, pp. 299–330.
Marquer, L., Otto, T., 2020. Microscopic Charcoal Signal in Archaeological Contexts. In: Henry, A.G. (Ed.), Handbook for the Analysis of Micro-Particles in Archaeological Samples. Springer, pp. 225–254.
Martín-Seijo, M., 2024. The presence of decayed wood in iron age contexts of northwest Iberia: wood-borer galleries and fungal hyphae. Environ. Archaeol. 29 (1), 34–50.
Martín-Seijo, M., Teira-Brión, A., Currás, A., Rodríguez-Rellán, C., 2020. After the fire: the end of a house life-cycle at the Iron age site of nabás (North-western Iberia). Veg. Hist. Archaeobotany 29, 427–446.
Matthews, W., 2016. Humans and fire: changing relations in early agricultural and built environments in the Zagros, Iran, Iraq. Anthr. Rev. 3, 107–139. https://doi.org/10.1177/2053019616636134.
Matthews, W., 2010. Geoarchaeology and taphonomy of plant remains and microarchaeological residues in early urban environments in the Ancient Near East. Quat. Int. 214, 98–113. https://doi.org/10.1016/j.quaint.2009.10.019.
Matthews, W., 2005. Micromorphological and microstratigraphic traces of uses and concepts of space. In: Hodder, I. (Ed.), Inhabiting Çatalhöyük: Reports from the 1995–1999 Seasons. McDonald Institute for Archaeological Research and British Institute of Archaeology at Ankara, Cambridge, pp. 355–398.
Mentzer, S.M., 2014. Microarchaeological approaches to the identification and interpretation of combustion features in prehistoric archaeological sites. J. Archaeol. Method Theory 21, 616–668.
Moore, J.D., 2012. The Prehistory of Home. University of California Press, Berkerley.
Murray, T., 1999. Time and Archaeology, first ed. Routledge, London, England.
Namdar, D., Zukerman, A., Maeir, A.M., et al., 2011. The 9th century BCE destruction layer at tell es-Safi/Gath, Israel: integrating macro- and microarchaeology. J. Archaeol. Sci. 38, 3471–3482. https://doi.org/10.1016/j.jas.2011.08.009.
Nicosia, C., Stoops, G., 2017. Archaeological Soil and Sediment Micromorphology. John Wiley & Sons, Oxford.
Palol P, Wattenberg F (1974) Carta arqueológica de España: Valladolid. Servicio de Publicaciones de la Diputación Provincial de Valladolid, Valladolid.
Pastor Quiles M (2021) Procesos constructivos y edificación con tierra durante la Prehistoria reciente en las tierras meridionales valencianas. Museu de Prehistòria de València.
Regev, L., Cabanes, D., Homsher, R., et al., 2015. Geoarchaeological Investigation in a Domestic Iron Age Quarter, Tel Megiddo, Israel. Bull Am Schools Orient Res 374, 135–157. https://doi.org/10.5615/bullamerschoorie.374.0135.
Romankiewicz, T., 2023. The building blocks of circular economies: rethinking prehistoric turf architecture through archaeological and architectural analysis. Open Archaeol. 9. https://doi.org/10.1515/opar-2022-0331.
Runjajić, M., Garfinkel, Y., Hasel, M.G., et al., 2023. Fire at the gate of Hazor: a micro-geoarchaeological study of the depositional history of a Bronze Age City gate. J. Archaeol. Sci. Rep. 49, 103914. https://doi.org/10.1016/j.jasrep.2023.103914.
Russell, N., Wright, K.I., Carter, T., Ketchum, S., Ryan, P., Yalman, N., Regan, R., Stevanović, M., Milić, M., 2014. Bringing down the house: house closing deposits at Çatalhöyük. In: Hodder, I. (Ed.), *Integrating Çatalhöyük*. Cotsen Institute of Archaeology Press, Los Angeles, pp. 109–121.
Sánchez Polo A (2021) Una cotidianeidad ritualizada: Formas de racionalidad prehistórica durante el Bronce Medio en la Submeseta Norte. Universidad de Salamanca.
Sánchez-Polo, A., Blanco-González, A., 2014. Death, Relics, and the Demise of Huts: patterns of Planned Abandonment in Middle BA Central Iberia. Eur. J. Archaeol. 17, 4–26. https://doi.org/10.1179/1461957113Y.0000000048.

Sánchez-Romero, L., Benito-Calvo, A., Rios-Garaizar, J., 2021. Defining and characterising clusters in Palaeolithic sites: a review of methods and constraints. J. Archaeol. Method Theory 29, 305–333. https://doi.org/10.1007/s10816-021-09524-8.

Santisteban, J.I., Mediavilla, R., López-Pamo, E., et al., 2004. Loss on ignition: a qualitative or quantitative method for organic matter and carbonate mineral content in sediments? J. Paleolimnol. 32, 287–299. https://doi.org/10.1023/B:JOPL.0000042999.30131.5b.

Sapir, Y., Avraham, A., Faust, A., 2018. Mud-brick composition, archeological phasing and pre-planning in Iron Age structures: Tel 'Eton (Israel) as a test-case. Archaeol. Anthropol. Sci. 10, 337–350. https://doi.org/10.1007/s12520-016-0350-z.

Schweingruber, FH (1990) Anatomy of European Woods. An atlas for the identification of European trees, shrubs and dwarf shrubs. Stuttgart: Paul Haupt.

Schiffer, M.B., 1985. Is there a "Pompeii Premise" in Archaeology? J. Anthropol. Res. 41, 18–41. https://doi.org/10.1086/jar.41.1.3630269.

Schiffer, M.B., 2003. Properties, performance characteristics and behavioural theory in the study of technology. Archaeometry 45, 169–171.

Schiffer, M.B., Skibo, J.M., Griffitts, J.L., et al., 2001. Behavioral archaeology and the study of technology. Am. Antiq. 66, 729–737.

Seco, M., Treceño, F.J., 1993. La temprana "iberización" de las tierras del sur del Duero a través de la secuencia de "La Mota". Medina del Campo (Valladolid). In: Arqueología Vaccea. Estudios Sobre El Mundo Prerromano En La Cuenca Media Del Duero. Junta De Castilla y León, Valladolid, pp. 133–172.

Shaffer, G.D., 1993. An archaeomagnetic study of a wattle and daub building collapse. J. Field Archaeol. 20, 59–75. https://doi.org/10.1179/009346993791974334.

Shahack-Gross, R., 2020. Destruction Layers, Near East/Southern Levant. In: Gilbert, A. S., Goldberg, P., Mandel, R.D., Aldeias, V. (Eds.), Encyclopedia of Geoarchaeology. Springer International Publishing, Cham, pp. 1–7.

Shalom, N., Vaknin, Y., Shaar, R., et al., 2023. Destruction by fire: Reconstructing the evidence of the 586 BCE Babylonian destruction in a monumental building in Jerusalem. J. Archaeol. Sci. 157, 105823. https://doi.org/10.1016/j.jas.2023.105823.

Sillar, B., Tite, M.S., 2000. The challenge of "technological choices" for materials science approaches in archaeology. Archaeometry 42, 2–20. https://doi.org/10.1111/j.1475-4754.2000.tb00863.x.

Skibo, J.M., Schiffer, M.B., 2008. People and Things: A Behavioral Approach to Material Culture. Springer Press, New York.

Smith, P.E.L., 1990. Architectural innovation and experimentation at Ganj Dareh. Iran. World Archaeol 21, 323–335. https://doi.org/10.1080/00438243.1990.9980111.

Springer C (2009). Tracking Identity in a Harrison Valley Pithouse. MA Thesis. Simon Fraser University. http://summit.sfu.ca/item/9798.

Stacey, F.D., 1967. The Koenigsberger ratio and the nature of thermoremanence in igneous rocks. Earth Planet Sci. Lett. 2, 67–68. https://doi.org/10.1016/0012-821x(67)90174-4.

Stevanović, M., 1997. The age of clay: the social dynamics of house destruction. J. Anthropol. Archaeol. 16, 334–395. https://doi.org/10.1006/jaar.1997.0310.

Stoops, G., 2003. Guidelines for analysis and description of soil and regolith thin sections. Soil Science Society of America, Madison.

Tabachnikov, S., Timorin, V., 2013. Osculating curves: around the Tait-Kneser Theorem. Math Intelligencer 35. https://doi.org/10.1007/s00283-012-9336-6.

Taylor J, Bogaard A, Carter T, Charles M, Haddow S, Knüsel CJ, Mazzucato C, Mulville J, Tsoraki C, Tung B, Twiss K (2017) 'Up in flames': a visual exploration of a burnt building at Çatalhöyük in GIS. In: Hodder I (ed) *Assembling Çatalhöyük*. Routledge, pp 127–149. https://doi.org/10.4324/9781351190992-11.

Tomé, L., Iriarte, E., Blanco-González, A., et al., 2024a. Searching for traces of human activity in earthen floor sequences: high-resolution geoarchaeological analyses at an Early Iron Age village in Central Iberia. J. Archaeol. Sci. 161, 105897. https://doi.org/10.1016/j.jas.2023.105897.

Tomé, L., Iriarte, E., Blanco-González, A., et al., 2024b. Fire use and waste management in an Iberian Iron Age village: Geoarchaeological insights into midden formation processes. J. Archaeol. Sci. Rep. 59, 104773. https://doi.org/10.1016/j.jasrep.2024.104773.

Tringham, R., 2013. Destruction of Places by Fire: Domicide or Domithanasia. In: Driessen, J. (Ed.), Destruction: Archaeological, Philological and Historical Perspectives. Presses universitaires de Louvain, Louvain-la-Neuve, pp. 85–103.

Tringham, R., Brukner, B., Kaiser, T., et al., 1992. Excavations at Opovo, 1985–1987: socioeconomic change in the Balkan Neolithic. J. Field Archaeol. 19, 351–386. https://doi.org/10.1179/009346992791548860.

Twiss, K.C., Bogaard, A., Bogdan, D., et al., 2008. Arson or accident? The burning of a Neolithic House at Çatalhöyük, Turkey. J. Field Archaeol. 33, 41–57.

Webley, L., 2007. Using and abandoning roundhouses: a reinterpretation of the evidence from Late Bronze Age–Early Iron Age Southern England. Oxf. J. Archaeol. 26, 127–144. https://doi.org/10.1111/j.1468-0092.2007.00277.x.

Wright, D., Kim, J., Park, J., et al., 2020. Spatial modeling of archaeological site locations based on summed probability distributions and hot-spot analyses: a case study from the three Kingdoms Period, Korea. J. Archaeol. Sci. 113, 105036. https://doi.org/10.1016/j.jas.2019.105036.